Ocean and Coastal Management 249 (2024) 106980

Contents lists available at ScienceDirect

Ocean and Coastal Management

journal homepage: www.elsevier.com/locate/ocecoaman

# Incorporating ecosystem services into comparative vulnerability and risk assessments in the Pearl River and Yangtze River Deltas, China

Yuting Peng *, Natalie Welden, Fabrice G. Renaud

*School of Social & Environmental Sustainability, University of Glasgow Dumfries Campus, Rutherford/McCowan Building, the Crichton, Dumfries, DG1 4ZL, UK*

ARTICLE INFO

*Keywords:*
Natural hazards
Social-ecological systems (SES)
Indicator-based approach
Ecosystem services
Risk reduction and management
Analytic hierarchy process (AHP)

ABSTRACT

Coastal river deltas face high risks from multiple natural hazards due to the combined effects of human activities, natural processes, and climate change. Vulnerability and risk assessments are essential for reducing and managing risks and, in the process, contribute to sustainable development. Despite adopting a social-ecological and multi-hazard perspective, previous risk assessments failed to achieve balanced consideration of both social and ecological sub-systems. To address this gap, we used an integrated risk assessment framework which incorporates the role of ecosystem services (ES) as a core component. A modular indicator library of ES indicators relevant to coastal river deltas was used to characterize multi-risks in the Pearl and Yangtze River deltas. Results indicate a higher risk level in the Pearl River Delta, with the key drivers of vulnerability and risk varying with scales. Visualizing hazard-prone and highly vulnerable areas facilitates the implementation of targeted management measures and policies to reduce disaster risks from natural hazards. Ecosystem services have been identified as important factors of the risk profiles, and their inclusion in risk reduction strategies ensures that policies can be put in place that allow ecosystems to provide services sustainably to communities.

## 1. Introduction

Coastal river deltas are low-lying landforms shaped by sediment transport processes under the interaction of fluvial and marine dynamics (Anthony, 2015; Dalrymple and Choi, 2007). With abundant natural resource availability, deltas are of high economic and ecological importance on a global scale and have become important for agriculture, urbanization and other human activities (Syvitski et al., 2009). Therefore, deltas should be regarded as dynamically coupled social-ecological systems (SES) (Hoitink et al., 2020; Twilley et al., 2016; Zhang et al., 2022). The current evolution of deltas is affected by the combined effects of human activities, such as the construction of upstream dams and coastal dikes, river management decisions, and urban expansion. Meanwhile, these anthropogenic changes generate a series of environmental impacts, including sediment erosion, land subsidence, sea level rise, and increased vulnerability of SES to multiple natural hazards (Giosan et al., 2014; Nicholls and Cazenave, 2010; Syvitski et al., 2009).

The increase in recorded disasters from natural hazards during the past two decades compared to 1980–1999 was largely due to a significant increase in climate-related disasters, affecting over 4 billion people and causing nearly $2.97 trillion in global economic losses (CRED, 2020). Climate-related disasters increased by more than 82% from 3656 in 1980–1990 to 6681 in 2000–2019, with floods and storm surge events accounting for 70% of these (CRED, 2020). As hotspots of global climate change, combined with dynamic landscapes, high population density and intense pressure caused by human interventions, deltas are facing growing risks resulting from natural hazards such as hydrological (floods), meteorological (storms) and climatological (drought) events (Tessler et al., 2015). Reducing and managing risks as well as achieving sustainable development in deltas is a global challenge and aligns with the calls of the Sendai Framework for Disaster Risk Reduction 2015–2030 and the 2030 Agenda for Sustainable Development (17 Sustainable Development Goals, SDGs) (Brondizio et al., 2016a; Cremin et al., 2023).

Risk assessment aims to identify and characterize areas exposed and vulnerable to natural hazards and is an essential step in hazard prevention and mitigation (Anelli et al., 2022; Chen et al., 2021). This can simplify the risk management process at local, regional and national levels, not only facilitating the implementation of targeted risk mitigation measures to protect the existing environments but also supporting the development of long-term risk prevention strategies (Gallina et al., 2016; Sebesvari et al., 2016). Research has increased in recent years,

* Corresponding author.
*E-mail addresses:* 2357444p@student.gla.ac.uk (Y. Peng), Natalie.Welden@glasgow.ac.uk (N. Welden), Fabrice.Renaud@glasgow.ac.uk (F.G. Renaud).

https://doi.org/10.1016/j.ocecoaman.2023.106980
Received 6 July 2023; Received in revised form 5 December 2023; Accepted 10 December 2023
Available online 26 December 2023

focusing on using risk assessment to map how regional environments are threatened by multiple hazards, including socio-economic vulnerability analysis (Berrouet et al., 2019; Cutter et al., 2003; Kirby et al., 2019; Su et al., 2015; Yang et al., 2019), biophysical perspective on hazard formation and potential exposures (Dewan, 2013; Yang et al., 2015), and comprehensive assessments by capturing the coupled perspective of social and ecological system (SES) (Anderson et al., 2021; Chang et al., 2021; Depietri, 2020; Hagenlocher et al., 2018; Lozoya et al., 2015; Tessler et al., 2015).

While vulnerability and risk assessments have traditionally focused on the socioeconomic contexts when addressing vulnerability of social systems, natural hazard events also threaten human livelihoods and health by disrupting the supply of natural resources and the stability of ecosystems (Ng et al., 2019; Rangel-Buitrago et al., 2020). When natural hazards occur, all ecosystems in deltas and various ecosystem services are affected. In particular, the primary sector (represented by extractive activities such as agriculture, which is crucial for food production in delta regions), is extremely vulnerable to the direct impact of natural hazards (Brondizio et al., 2016a). Additionally, services such as soil quality, erosion control and climate regulation are linked not only to biomass production, but are also integral to coastal adaptation and risk reduction, such as coastal erosion management strategies (Gracia et al., 2018). Considering SES in risk assessments is therefore a new general trend (Brondizio et al., 2016b; Gracia et al., 2018). Reviews by Sebesvari et al. (2016) and Hagenlocher et al. (2019) both revealed that risk assessment studies predominantly focused on social dimensions of risk with inadequate consideration of ecological and environmental aspects, even in SES-based studies. To characterize better the inter-relationship of social and ecological systems, incorporating the concept of ecosystem services into risk assessment can help integrate the various components of the biophysical, ecological, social, and economic environments (Armatas et al., 2017; Collins et al., 2011; Peng et al., 2023).

The complex and interdependent characteristics of natural hazards mean it is impossible to address single risks in isolation (IPCC, 2022; Nhamo et al., 2018). Risk assessments to single hazards fail to provide a comprehensive profile of the multiple risks stemming from various natural and anthropogenic forces (Gallina et al., 2016), which can materialise simultaneously or in a cascading pattern. Recognizing the diverse range of natural hazards and climate change impacts in deltaic environments underscores the necessity of assessing multiple risks and presenting a comprehensive multi-risk profile (Hagenlocher et al., 2018; Tessler et al., 2015). Consequently, adopting a multi-hazard risk perspective that accounts for the spatial scales of multiple hazards is crucial in devising efficient risk reduction and adaptation strategies (IPCC, 2022).

As a coastal nation whose landmass covers a large geographic range, multiple climatic regions and ecotypes, China is severely affected by numerous environmental disasters. The country is ranked among the top ten countries globally most affected by natural hazard-related disasters over the period from 2000 to 2019, in terms of hazardous event occurrences, economic losses, and human casualties, as shown by data from the Emergency Events Database (EM-DAT) (CRED, 2020). Notably, southern China (Pearl River Delta) and eastern China (Yangtze River Delta) have experienced a particularly high incidence of flooding events (Kundzewicz et al., 2019). Therefore, flood risk analysis for the Yangtze or Pearl River Delta and even China as a whole has received the most attention and included studies focusing on model-based flood hazard assessment and prediction (Fang et al., 2020; Lin et al., 2020; Xu et al., 2014; Yin et al., 2020; Zhang et al., 2014; Zhao et al., 2021), and vulnerability and risk assessments of flooding (Chen et al., 2021; Jian et al., 2021; Sun et al., 2022; Yang et al., 2015). In addition, there are vulnerability or risk assessments for other single hazards, encompassing cyclones (Sajjad et al., 2020; Yin et al., 2013; Zhang et al., 2017; Zhou et al., 2021), storm surges (Li and Li, 2011; Lilai et al., 2016; Xianwu et al., 2020), drought (Chen et al., 2016), and pollution (Liang et al., 2022; Zhu et al., 2019). Previous studies of risk assessments in China also lacked an SES perspective, with the emphasis being either on social vulnerability or the exclusive assessment thereof (Ge et al., 2013, 2017; Sun et al., 2019; Yang et al., 2019; Yu et al., 2018). Currently, there is inadequate documentation of integrated vulnerability and risk assessments to multi-hazards in these two deltas. In the Yangtze River Delta, Liu et al. (2013) mapped the exceedance probability distribution of typhoons and flood hazards to human casualties. In another research, the Global Delta Risk Index was computed to better identify green infrastructure prioritization in part of the Yangtze River Delta (Ou et al., 2022). The research predominantly focused on green infrastructure, and lacked the inclusion of hazard magnitude and local knowledge to determine diverse dimensions of SES vulnerability, particularly those hazard-dependent indicators. Consequently, multi-hazard risk assessments are needed, encompassing not only the whole Pearl and Yangtze River deltas but also an exploration of regional disparities across both of these deltaic environments.

Addressing the above-mentioned gaps, we developed a multi-hazard risk index for deltas from an integrated perspective of human, economic, and environmental dimensions through a conceptual framework and modular indicator-based tools. This study involved the systematic integration of ecosystem services to address the inter-relation between social and ecological systems, using a combination of quantitative and qualitative approaches to describe coupled SES dynamics for deltas. The application of the new framework aims to assess the vulnerability and risks to multiple hazards in the Pearl River Delta and Yangtze River Delta, and to understand their regional differences. In this paper we (1) determine the overall vulnerability and risk profile of the Pearl and Yangtze River deltas; (2) assess which regions in these deltas are at higher risk levels to natural hazards, and how these differ within and across deltas; and (3) we evaluate how ecosystem services affect vulnerability and risk, and how ecosystem service indicators can contribute to improved risk management.

## 2. Materials and methods

### 2.1. Study areas

The Pearl River Delta (PRD) has a total land area of 55,000 km$^2$ and a population of 64 million, which is only located in Guangdong Province (Fig. 1) (PSB, 2019). The population density of the delta is 1172 persons/km$^2$, which is significantly higher than both China's average, and that of the Yangtze River Delta (YRD) (Table 1). It has become the world's largest metropolitan area in both size and population (The World Bank, 2015). From July to September, an annual average of 7–9 typhoons land in the eastern and southern coastal areas of China (CMA, 2014). From 2011 to 2020, the average direct loss from storm surges in

**Table 1**
*Comparison of biophysical and social characteristics between China, PRD and YRD. Source:* NBS (2020).

| | | China | PRD | YRD |
|---|---|---|---|---|
| Biophysical | Land area (km$^2$) | 9.6 million | 55,000 (0.6% of China's total land area) | 225,000 (2.3% of China's total land area) |
| | Climate | Diverse climate due to its vast territory | Subtropical monsoon climate with abundant rainfall and high humidity | |
| Social | Population (million) | 1400 | 64 (4.6% of China's total population) | 136 (9.7% of China's total population) |
| | Population density (person/km$^2$) | 148 | 1172 | 750 |
| | GDP (billion US$) | 14,306 | 1258 (8.8% of China's total GDP) | 2952 (20.6% of China's total GDP) |

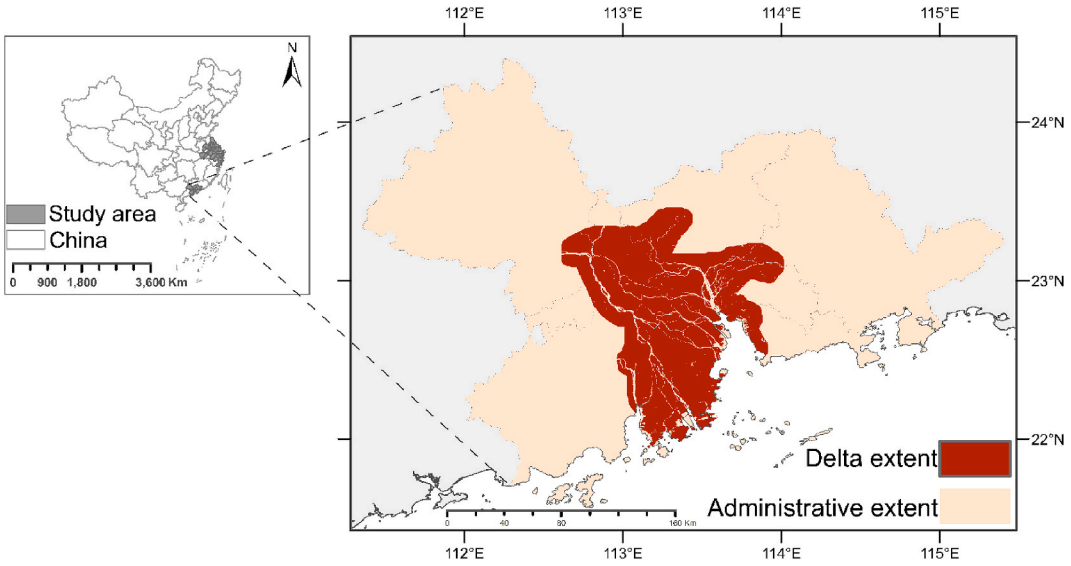


**Fig. 1.** *Map of Pearl River Delta. The administrative tracts are marked in yellow and represent the study areas. Data from GADM (2018). Red areas show the extent of the delta (data from Tessler et al. (2015), based on geographical characteristics and remote sensing images).*

the PRD alone was as high as US$433.5 million per year, exceeding the YRD (MNR, 2021). Besides, the PRD region is identified as a significant risk hotspot to tropical cyclones (typhoons), requiring the implementation of urgent risk reduction and management strategies (Sajjad et al., 2020).

The YRD is a relatively developed economic region in the eastern coastal areas of China (Fig. 2). This study adopts the definition of the core region in the Outline of the Yangtze River Delta Regional Integrated Development Plan, consisting of Shanghai, 9 cities in Jiangsu Province, 9 cities in Zhejiang Province and 8 cities in Anhui Province, with an area of 225,000 $km^2$ (The CPC Central Committee and General Office of the State Council, 2019). The city cluster, led by Shanghai, has been recognized as one of the six major urban belts in the world (NBS, 2004). As an agricultural and industrial centre, the Yangtze River Delta comprises 2.3% of the area and about 9.7% of the population of China; as of 2019, the region has generated nearly 20.6% of China's total Gross Domestic Product (GDP) (Table 1). The Yangtze River Delta is vulnerable to multiple natural hazards such as typhoons, flooding, and storm surges due to its geographical location (Ge et al., 2013). According to the Bulletin of China Marine Disaster (MNR, 2021), the average direct economic loss from 2011 to 2020 caused by storm surges is about US $297.7 million per year.

Managing the risks faced by the delta regions with their distinct demographic and economic disparities from the rest of China is critical to achieving sustainable development. Furthermore, understanding the regional risk differences between the PRD and YRD helps to identify the key drivers causing the final multi-risk, then formulating goal-oriented adaptation and risk reduction measures.

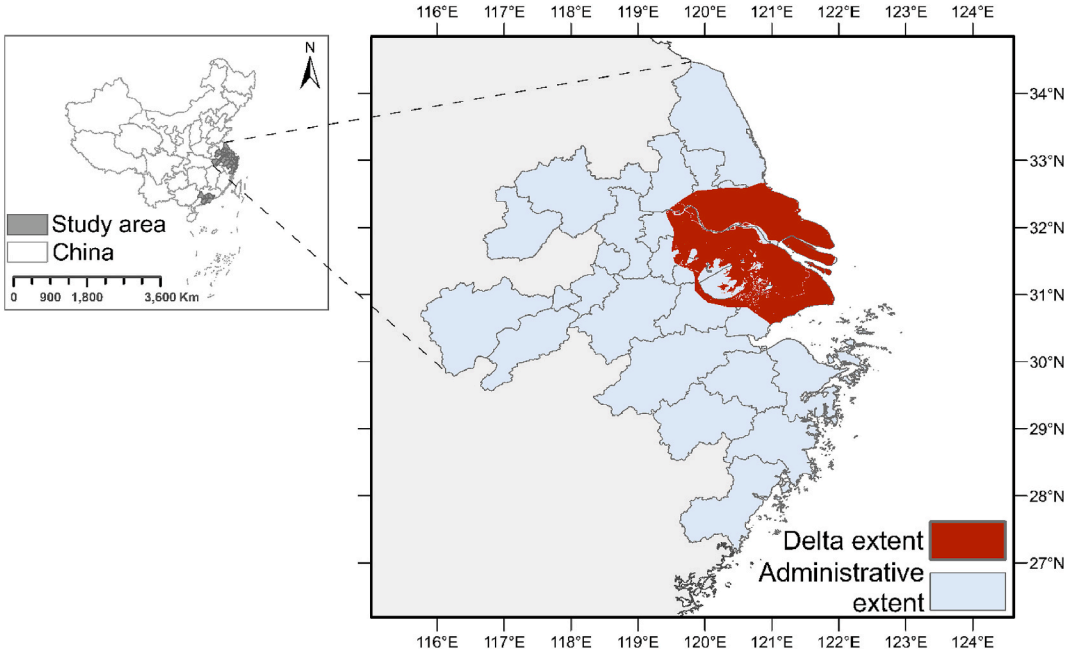


**Fig. 2.** *Map of Yangtze River Delta. The administrative tracts are marked in blue and represent the study areas. Data from GADM (2018). Red areas show the extent of the delta (data from Tessler et al. (2015), based on geographical characteristics and remote sensing images).*

### 2.2. Research design

#### 2.2.1. Risk framework

This study applies a comprehensive research framework (Delta-ES-SES) for deltaic SES vulnerability and risk assessment (Peng et al., 2023), which was adapted from Sebesvari et al. (2016). The adapted framework integrates various risk components (Risk = Hazard × Exposure × Vulnerability) from the spatial perspective of the SES and can be applied to single and multiple hazards (Fig. 3). This modular structure establishes the linkage between ecosystem services and vulnerability, taking into account the social, ecosystem, and ecosystem service dimensions of vulnerability. The indicator-based methodology linked to different levels of the indicator library can be easily adjusted for different research priorities and assigning weights, which is applicable to the characteristics of delta environments and enables intra-delta and cross-delta comparisons.

#### 2.2.2. Risk components and data collection

Focusing on differences in disaster risk levels across deltas, we used datasets at various scales representing multiple factors contributing to the vulnerability and risk profile of deltas for further analysis and integration. Considering data availability, we assessed the multi-hazard risks by administrative unit (city-level). The Delta-ES-SES framework classifies risk into hazard, exposure and vulnerability components, with additional sub-components. It also allows calculating and comparing single hazard risk and identifying the main drivers of final risk scores. Supplementary Material 1 provides an overview of the detailed information and data processing steps of indicators for each component that can be used to support future studies.

*2.2.2.1. Hazard and exposure.* This study mainly considers four types of natural hazards (IFRC, 2022): (1) Hydrological (flooding), (2) Meteorological (cyclones and storm surges), (3) Climatological (drought) and (4) Mixed (salinity intrusion). The selection criteria of hazard indicators (flooding, cyclone, storm surges, and salinity) are spatial data that can be mapped in a GIS environment (tool: Arc-GIS version 10.8), using a wide variety of data sources from international organizations and publishing papers (Table 2). As for drought, based on the precipitation and

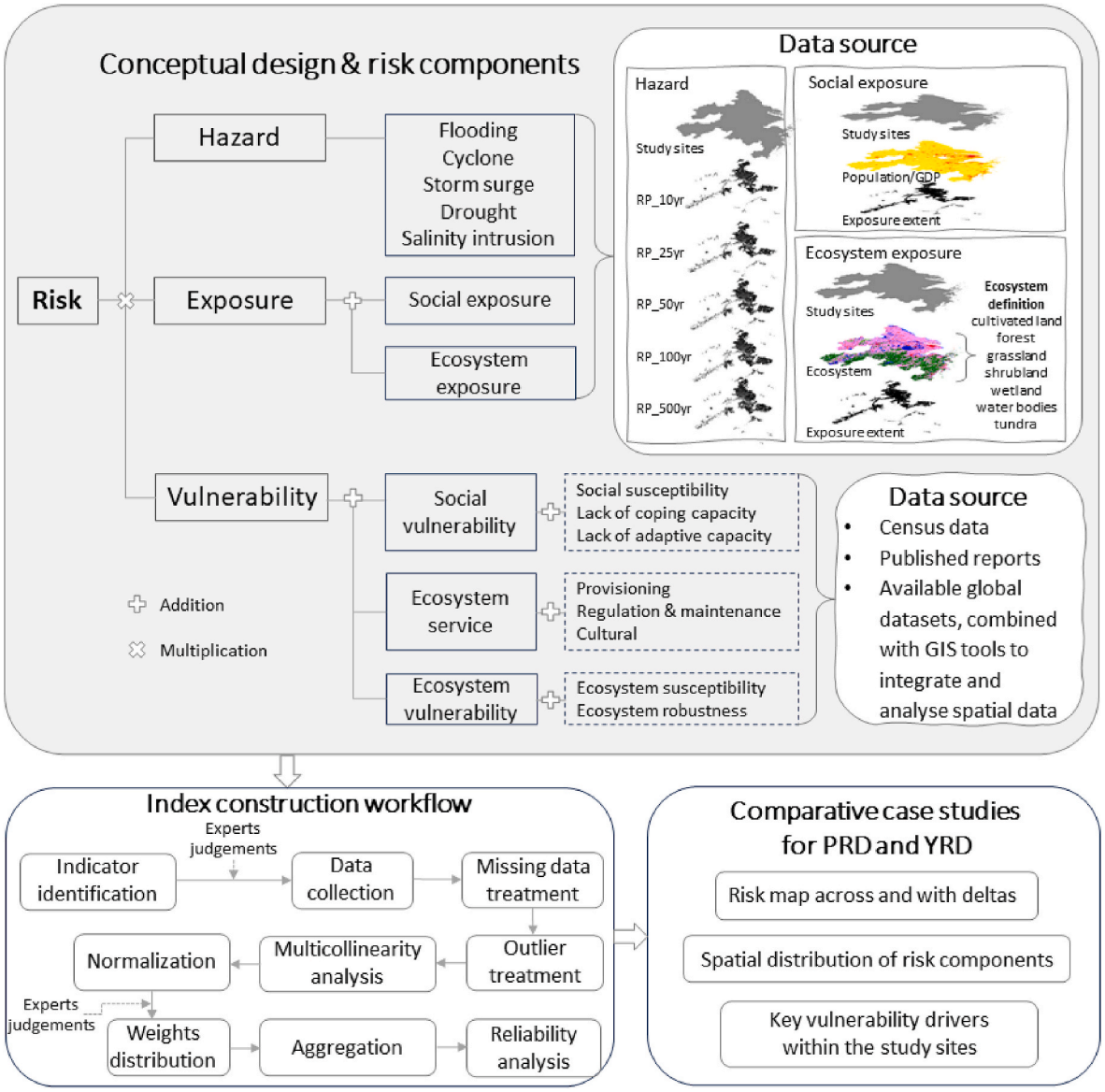


**Fig. 3.** Schematic conceptual and methodological structure of the Delta-ES-SES risk framework. The data source for hazard and exposure (the upper right) mainly shows the data acquisition process taking the flooding in the Yangtze River Delta as an example. RP_10yr to RP_500yr refer to different return period maps of floods. Detailed information for each indicator is included in Supplementary Material 1.

**Table 2**
Indicators, data type and sources used for hazard and exposure components.

| Category | Indicator | Time Period | Data Source |
|---|---|---|---|
| **Hazard** | | | |
| Flooding | Mean water depth (in m) | Return period: 10, 20, 50, 100, 500 years | Francesco et al. (2016) |
| Cyclone | Wind speed (km/h) Cyclone frequency | 1970–2009 | Peduzzi (2014) |
| Storm surge | Sea levels (in m) | Return period: 10, 25, 50, 100, 250, 500, 1000 years | Muis et al. (2016) |
| Drought | Standardized precipitation evapotranspiration index (SPEI) | 1979–2020 | Vicente-Serrano et al. (2010) |
| Salinity intrusion | Salinity (total dissolved solids; mg/l) | 1979–2010 | van Vliet et al. (2021) |
| **Exposure** | | | |
| Social Exposure | % of population exposed to each hazard | 2020 | WorldPop (2018) |
| | % of economics exposed to each hazard | 2019 | Xinliang (2017) |
| Ecosystem Exposure | Ecosystem exposed to each hazard (%) | 2020 | NGCC (2020) |

potential evapotranspiration data provided by the CCCS (2021) dataset from 1979 to 2020, spatially explicit data of drought score and frequency were developed for the study area by the Standardized Precipitation Evapotranspiration Index (SPEI) construction method introduced by Vicente-Serrano et al. (2010). Social exposure consists of the percentage of people and economics (GDP) exposed to these hazards, and ecosystem exposure is defined as the percentage of ecosystem area exposed to hazard, as Fig. 3 shows. These data are derived from the combination of hazard data and spatial data on population, economics and Land Use/Land Cover (LULC), respectively, resulting in the mean value for each administrative area.

*2.2.2.2. Vulnerability.* In this study, vulnerability is composed of (1) social vulnerability (social susceptibility, lack of coping and adaptive capacities), (2) ecosystem services (provisioning, regulation & maintenance, and cultural services), and (3) ecosystem vulnerability (ecosystem susceptibility and ecosystem robustness). A list of indicators was obtained by combining a systematic review of the deltaic SES-related ecosystem services literature and risk assessment papers (Peng et al., 2023), then identifying a series of hazard and vulnerability indicators for the YRD and PRD by inviting experts to fill out indicator questionnaires. Forty-two questionnaires were obtained from experts belonging to relevant academic institutions or government sectors in China, with knowledge of ecosystem conservation and restoration, ecology, climate change adaptation, land management and other related backgrounds. Vulnerability to different types of hazards could be different and can change over time (Gallina et al., 2016). Expert consultation not only distinguishes the directional effects of each vulnerability indicator with the hazard (increasing +/decreasing - vulnerability), but also adjusts the indicator for the study area. Data sources and time periods of indicator data availability vary, and are mainly obtained from census data, available global databases, as well as data from some published papers. The indicators "Forest Connectivity" and "Wetland Connectivity" are calculated from existing databases and GIS plugin (Saura and Torné, 2009). Finally, vulnerability is composed of 46% social vulnerability and 54% ecological (ecosystem service and ecosystem) indicators. Section 2.2.4 provides a specific list of vulnerability indicators and their associated weights, and Supplementary Material 1 provides information on data sources. Further information related to the consulted experts is provided in Supplementary Material 2.

Various indicators related to social vulnerability are determined from expert consultation to present the overall status of the social system under the context of vulnerability and risk assessment. This research divides indicators into three categories, namely indicators related to social susceptibility (11 indicators) and lack of coping (12 indicators) and adaptive capacity (3 indicators). Social vulnerability indicators are generally available through census data in China. Social susceptibility includes indicators related to key services (e.g. indicators 'access to irrigation') and economic and demographic characteristics, such as the indicator 'dependency ratio'. Coping capacity reflects the ability of humans to address and overcome the adverse impacts of hazards (IPCC, 2022), which is mainly divided into two aspects: individual & household and infrastructure & services. Adaptive capacity refers to the ability to reduce adverse risks and impacts, which is assessed by aspects of social and governmental management.

Ecosystem service indicators related to vulnerability are divided into provisioning (6 indicators), regulation & maintenance (12 indicators) and cultural services (3 indicators). Provisioning services, include indicators related to agricultural, forestry and aquaculture production and water resources, and jointly determine the ecosystem's ability to provide various materials or energy (Haines-Young and Potschin, 2018). Regulation and maintenance services mainly reflect beneficial effects on the human environment through biochemical or physical processes (Haines-Young and Potschin, 2018). This research considers soil quality regulation, erosion regulation, pollination, biodiversity, natural hazard protection, air quality regulation, climate regulation and water regulation. Indicators for cultural services are related to human habitation of landscapes and environments, and include the development of tourism and accessible recreation areas.

The ecosystem susceptibility to natural hazards indicates the degree of the ecosystems to be adversely affected (IPCC, 2022). Ecosystem susceptibility indicators are divided into habitat destruction (3 indicators: percentage of deforested area, percentage of wetland loss, and percentage of area covered by problem soils), habitat degradation (2 indicators: increased use of chemicals and fertilisers, Normalized Difference Vegetation Index) and habitat fragmentation (3 indicators: forest connectivity, wetland connectivity and river connectivity). Ecosystem robustness shows the ability of ecosystems to stabilise various ecological functions and respond to risks (Sebesvari et al., 2016), and includes two indicators: percentage of area of nature reserves and funding on environmental protection.

### 2.2.3. Data processing

The computed risk index supports a spatial analysis workflow. However, as there were no available spatial data for some indicators, this study mapped the risk at the administrative scale. For spatial datasets, statistical values (mean) for administrative areas were derived using the zonal tool in ArcGIS 10.8. As shown in Fig. 3, data processing included missing value analysis (mean values of surrounding areas) and outlier treatment, as detailed in Supplementary Material 2. Box plots were computed to detect the outliers of all data, where outliers were defined as data points that were located outside the whiskers of the box plot 1.5 * interquartile range. A winsorization or trimmed estimators approach was used to process the potential outliers after checking the data sources. The second step was to check for multicollinearity within each indicator domain. The Correlation Coefficient Kendall's tau_b was used in this analytical procedure (with Kendall's tau_b $> 0.9$ indicating collinearity) (Hagenlocher et al., 2018). After taking into account the data features and the aim of the composite indicator (Nardo et al., 2005), the rescaling (min-max normalization) method was applied to redistribute all indicators to a range with an average of zero and a standard deviation of one. Some indicator data were adjusted so that all high indicator values indicate high vulnerability and risk.

### 2.2.4. Aggregation method

This study weighted the risk components using a combination of

empirical evidence and the analytic hierarchy process (AHP and improved AHP). The AHP has been widely used in risk assessments to identify the relative importance of various associated indicators (Ouma and Tateishi, 2014; Pathan et al., 2022), which enables a better understanding of local environments (Ishizaka and Labib, 2011). Regardless of the delta environment settings, the drivers contributing to risks and final risk scores will be region-specific (Pathan et al., 2022). Given the geographic attributes of vulnerability and risk, a combination of stakeholder and scientific knowledge may improve risk assessment and disaster management (Morelli et al., 2021). Based on literature analysis and IPCC reports (2014), the risk components (hazard, exposure, and vulnerability) are calculated based on equal-weighted standardization. For the exposure and vulnerability subcomponents (indicators ≤3, see Fig. 3), we took the traditional AHP approach to develop pairwise comparison matrices for each component. Consistency ratios less than 0.10 are acceptable (Saaty, 2008). This standard AHP requires pairwise comparison, which is not much suitable for multi-indicator research, especially if there are more than 10 elements. It is time-consuming and may lead to inconsistent judgments. An improved AHP (IAHP) is therefore adopted to weigh the criteria of all vulnerability sub-components (within ecosystem vulnerability, ecosystem service and social vulnerability), which is to change the pairwise comparison to the ranking of the elements (Fengwei et al., 2013). The main step is to rank the indicators according to expert consultation. The most important indicator is assigned a value of 10, the least important is 1, and the values of other indicators are assigned values through linear interpolation based on the importance order. The other steps are the same as in standard AHP, calculating an eigenvector according to the comparison matrix, which is the final weight distribution. Fig. 4 presents the final distribution of weights in this study.

Finally, following the modular framework, the (multi-)hazard, exposure and vulnerability of the deltaic SES are aggregated by multiplicative aggregation into a (multi-hazard) risk index, that is,

$$RISK_{SES} = HAZ_{SES} * EXP_{SES} * VUL_{SES}$$

Where $HAZ_{SES}$ is the hazard score; $EXP_{SES}$ is the exposure score, which is calculated as

$$EXP_{SES} = \sum_{i=1}^{n} (w_i * EC_{SES})$$

Here $EC_{SES}$ is the different exposure component of SES where $w_i$ is the weight of each type of exposure indicator.

Besides, $VUL_{SES}$ is the vulnerability score of SES, which use the mean of three vulnerability domains (after combining the weights $w_j$), which is calculated using

$$VUL_{SES} = \sum_{j=1}^{n} (w_j * VD_{SES})$$

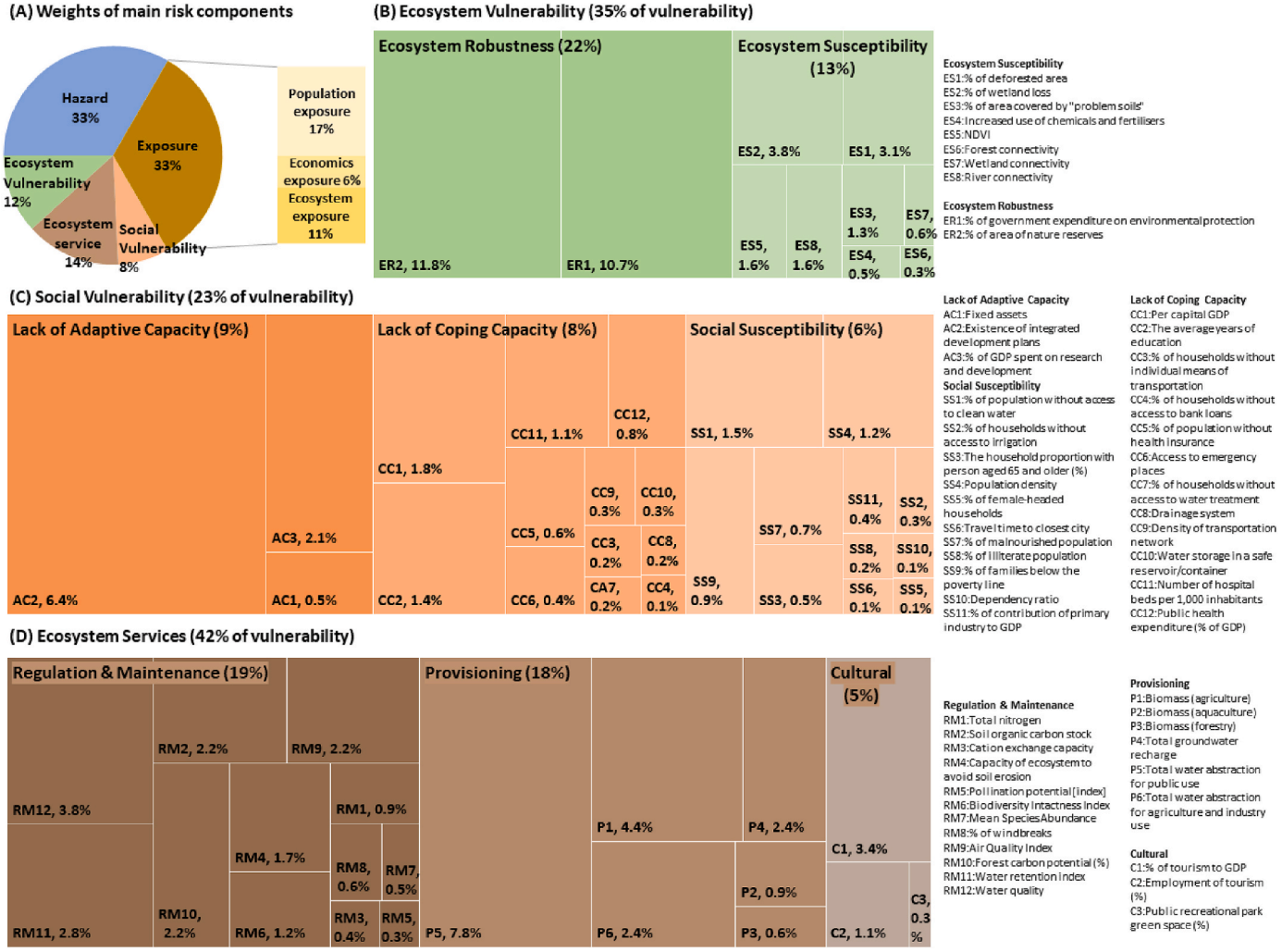


**Fig. 4.** Final distribution of weights across risk domains. (A) Hazard, Exposure, Vulnerability: equal weights (33%); Exposure and Vulnerability sub-components: AHP method; (B), (C), and (D) Weight assignment for sub-components (AHP method) and each vulnerability indicator (IAHP method). The percentages displayed in these three figures pertain to the vulnerability component.

$VD_{SES}$ refers to ecosystem vulnerability, ecosystem services, and social vulnerability, which is calculated using

$$VD_{SES} = \sum_{s=1}^{n} (w_s * VD_s)$$

where $w_s$ is the weights of indicators in the sub-component of vulnerability domain (VD) (e.g. indicators of ecosystem susceptibility and robustness). Here VD is calculated by the aggregation of each normalized indicator ($x_k^{'}$) with specific weights ($w_k$).

$$VD = \sum_{k=1}^{n} (w_k * x_k^{'})$$

Final outputs are visualized using ArcGIS 10.8 based on manual equal interval across deltas and quantile classification within the delta, respectively. Equal interval classification emphasizes the number of risk scores relative to other scores, which visualizes the absolute distribution

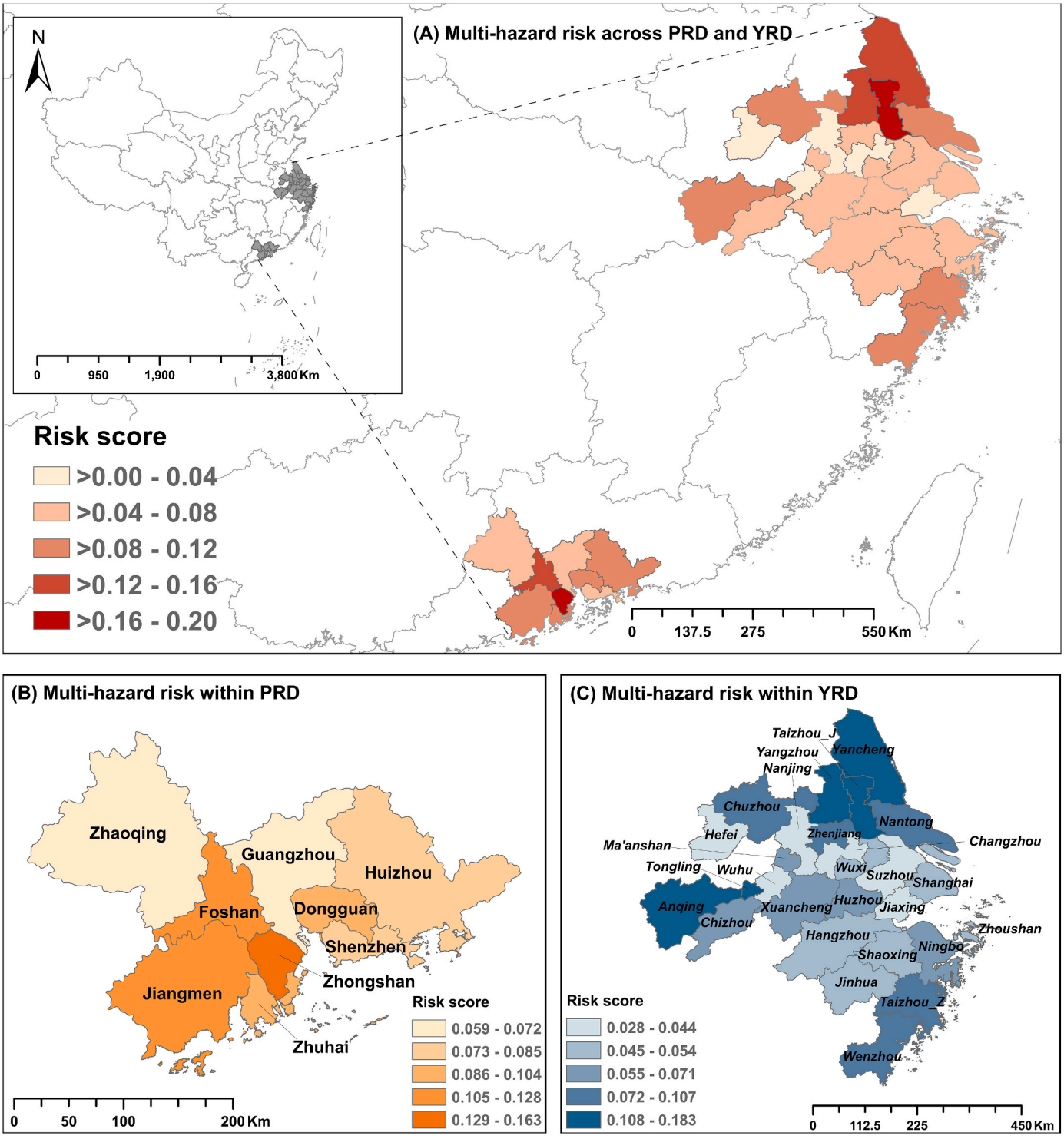


**Fig. 5.** (A) Multi-hazard risk across the deltas (risk score classification: equal interval); (B) and (C) Multi-hazard risk within the Pearl River Delta and Yangtze River Delta, respectively (risk score classification: quantile method). Note: the colours in (B) and (C) are not comparable, specific values are provided in the corresponding legends.

of risk values for all regions of the two deltas, allowing identification of regions with highest/lowest and closest distribution of risk scores. Meanwhile, the quantile classification assigns equal number of administrative units to each class, which could interpret the spatial patterns of relative risk scores within the delta. The processed data and aggregation methodology can be found in Supplementary Material 3.

#### 2.2.5. Reliability analysis

We applied the reliability index to examine the data quality used in this study, which is adjusted and developed by Hagenlocher et al. (2018) and Marin-Ferrer et al. (2017). It involves (1) percentage of missing data and outliers for vulnerability indicators, including any that have been estimated; (2) percentage of missing hazard data; (3) percentage of proxy indicators; and (4) percentage of indicator data at provincial level rather than city level. The final reliability index ranges from 0 to 100%, and the larger the number, the higher the reliability. Based on this approach, the reliability indices for the PRD and YRD are 83% and 82%, respectively, and details are provided in Supplementary Material 2.

## 3. Results

### 3.1. Multi-hazard risk of deltaic social-ecological systems

Using the Delta-ES-SES framework, we present the risk profiles from the multi-hazard risk assessment across the two coastal river deltas, with risk scores ranging from 0.028 to 0.183 (Fig. 5). About 42% of the 36 administrative tracts in the study area are at medium to high risk levels (risk score >0.08). Fig. 5(B) and C shows relative multi-hazard risk scores within the deltas, which are 0.059–0.163 for the PRD region and 0.028–0.183 for the YRD region. It can be seen from the data in Fig. 6 that the average risk to SES in the PRD (risk score 0.099) is higher than the YRD (risk score 0.071), and its hazard exposure is also higher than the average scores in the YRD. Compared to the YRD, all cities in the PRD are at medium to high risk.

High-risk cities are led by high hazard exposure and moderate to high vulnerability, including two cities with the highest risks: Taizhou_J (risk score 0.183) in the YRD and Zhongshan (risk score 0.163) in the PRD. Most cities in the PRD are characterized by moderate to high

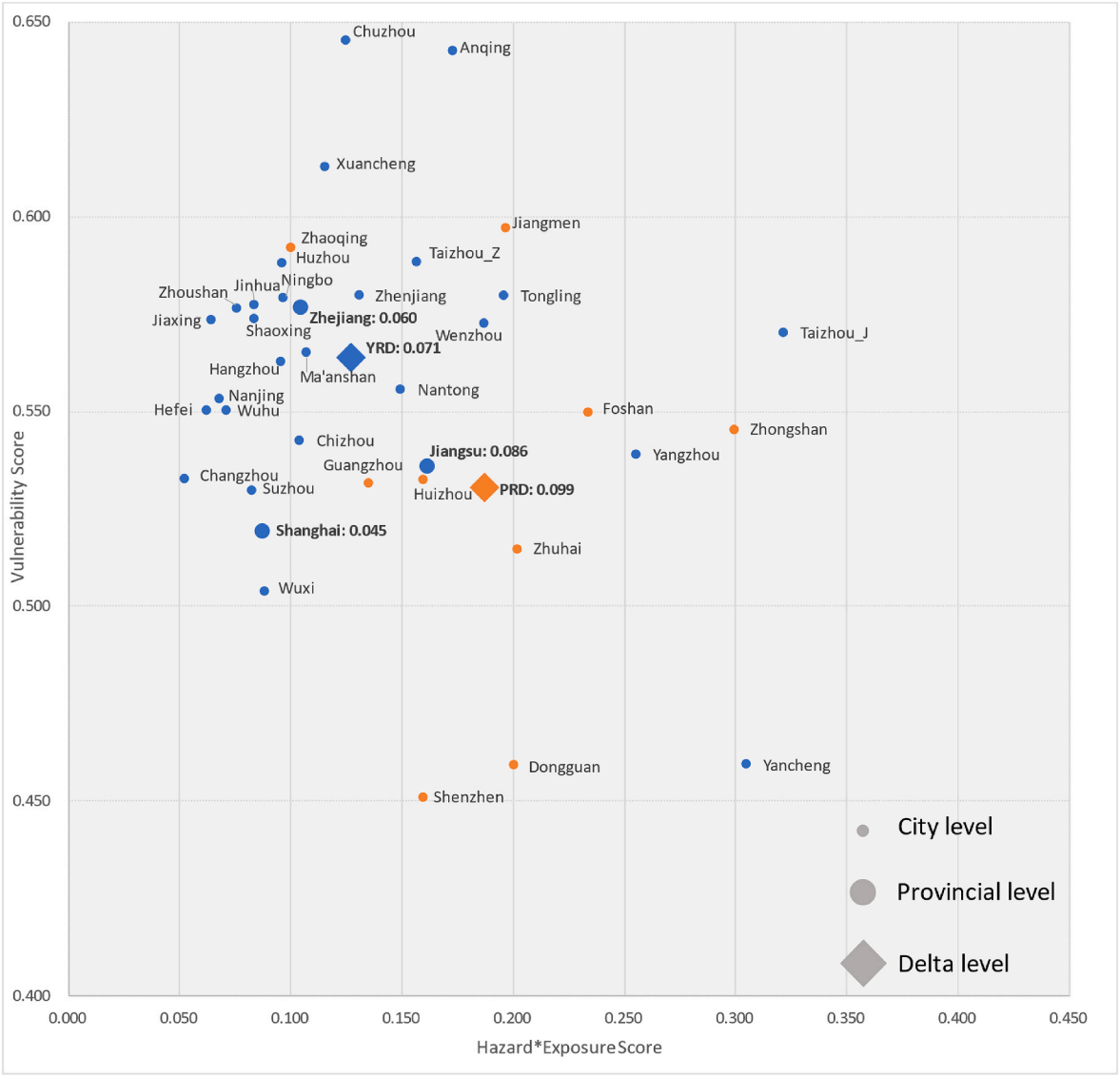


**Fig. 6.** Scatter plot of risk assessment results, showing the proxy indices for hazard*exposure and vulnerability used to estimate the risk indices, blue colour for Yangtze River Delta (YRD) tracts and orange colour for Pearl River Delta (PRD) tracts. Hazard*Exposure refers to the multiplication of hazard and exposure scores. Dot size represents different administrative units: city level, provincial level, and delta level. Taizhou_J and Taizhou_Z represent Taizhou in Jiangsu Province and Taizhou in Zhejiang Province, respectively.

vulnerability and moderate to high hazard exposure (orange dots in Fig. 6), except for Zhaoqing and Guangzhou. These two cities have lower multi-hazard exposure, which are located in the interior of the PRD, as shown in Fig. 5(B). The risk levels of YRD show large variability, as it is shared by four adjacent provinces (blue dots in medium size), with Jiangsu (risk score 0.086) having significantly higher average risk than Anhui (risk score 0.071), Zhejiang (risk score 0.060), and Shanghai (risk score 0.045). Low-risk cities have lower hazard exposure scores, are mainly located in central inland areas of the YRD, as shown in Fig. 5(C). Generally, cities with higher risk scores are mostly located in the northern and southern coastal areas, with moderate to high distribution of exposure to hazardous events. There are some exceptions, like Tongling and Anqing, which are in the interior of the YRD, and which have moderate to high risk levels. In order to understand the risk differences and their internal drivers across the study area, the risk components of the deltas are visualized separately (Fig. 7).

### 3.2. Risk component analysis

Overall, the PRD has higher multi-hazard exposure (mean value: 0.187) compared to the YRD (mean value: 0.127). The PRD is facing a high probability of hazardous events in the southern coastal regions, especially floods, cyclones and storm surges. The northeast coastal area of the YRD has the highest multi-hazard risk and is mainly affected by storm surges. There are also some areas in the western inland region that have higher multi-hazard risks because of the high exposure to drought, such as Anqing and Tongling.

The analysis further indicates internal differences between the different risk components of the two deltas, especially the final distribution of vulnerability, even when the risk levels are similar. From the data in Fig. 7, we can see that while the overall vulnerability difference between the two deltas is not high (0.530 in PRD and 0.564 in YRD), the scores of different vulnerability components vary. The ecosystem and ecosystem service vulnerability in the PRD is slightly higher than the YRD, with the social vulnerability score lower than the YRD. This is mainly due to the difference in the scores of lack of coping and adaptive capacity between the two deltas, which are largely driven by social development and economic conditions.

Results for social vulnerability show discrepancies between developed cities and less economically developed areas both across and within the deltas. Areas with higher social vulnerability, especially the western and northern YRD, are predominantly characterized by areas of lower economic development. Further analysis reveals that the spatial distribution of social vulnerability is mainly driven by the scores of coping and adaptive capacity sub-components. Generally, both the western PRD and the northern YRD show higher ecosystem

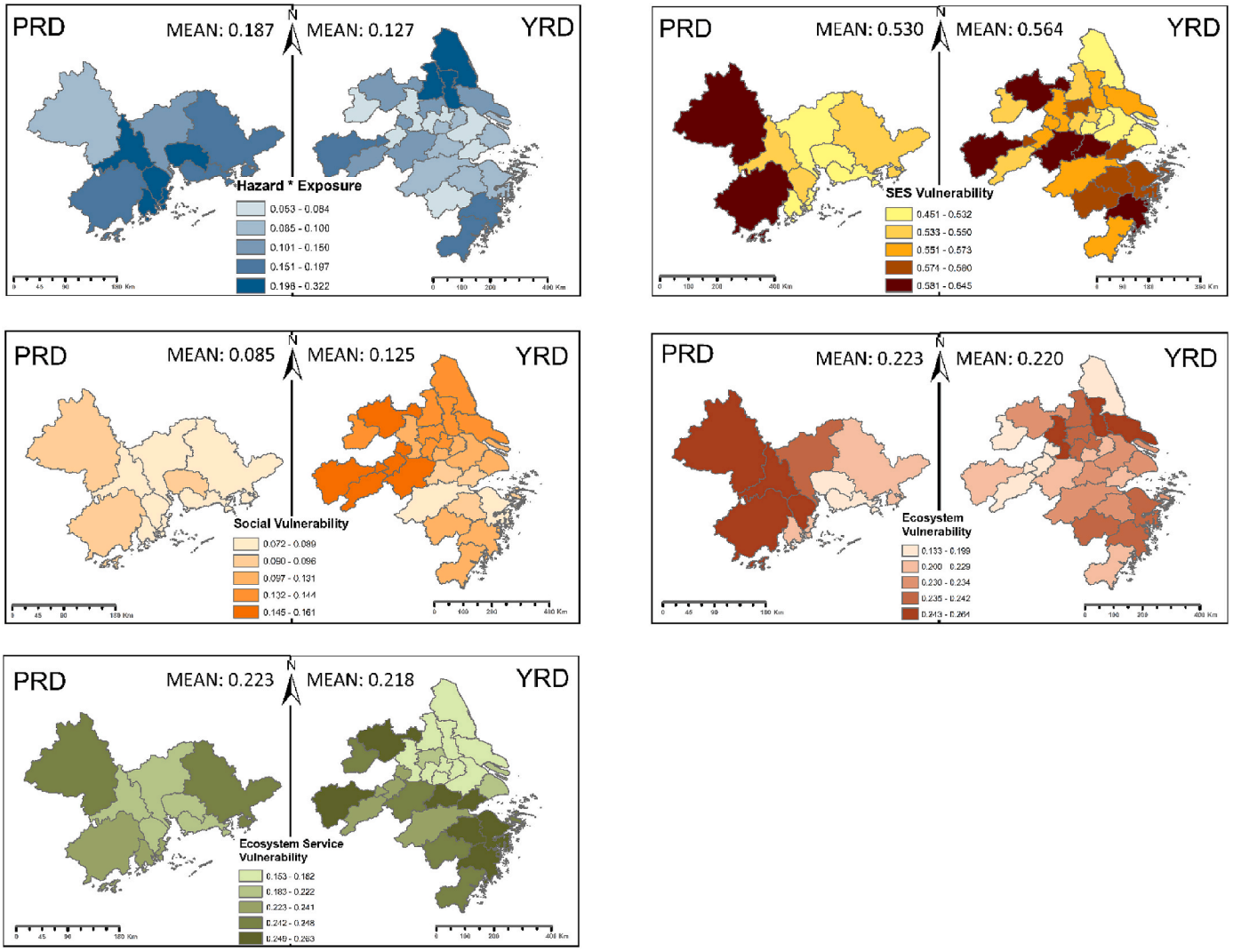


**Fig. 7.** SES Hazard*Exposure, SES Vulnerability, and corresponding scores of vulnerability domains for multi-hazards: Social vulnerability, Ecosystem vulnerability and Ecosystem service vulnerability. Score ranges are based on quantile classification. SES Hazard*Exposure refers to the multiplication of hazard and exposure scores.

vulnerability. Breaking down the ecosystem vulnerability into ecosystem susceptibility and ecosystem robustness reveals high overlaps between ecosystem vulnerability and robustness. Ecosystem susceptibility mainly contributes to the low to moderate levels of ecosystem vulnerability in the central YRD. As for the ecosystem service component, Zhaoqing and Huizhou in the PRD, as well as the western and southern YRD, show higher vulnerability scores. These higher scores are shaped by different sub-components; for instance, decomposed scores of provisioning, regulation & maintenance, and cultural services contribute predominantly to vulnerability scores in the southern YRD, Huizhou of PRD, and the western YRD, respectively.

Combining the spatial distribution of SES vulnerability with the other three components indicates spatial variations in the overlapping areas of final vulnerability and other components. Following Hagenlocher et al. (2018), we drew the relative contribution of vulnerability in the two deltas (Fig. 8), which allows the identification of

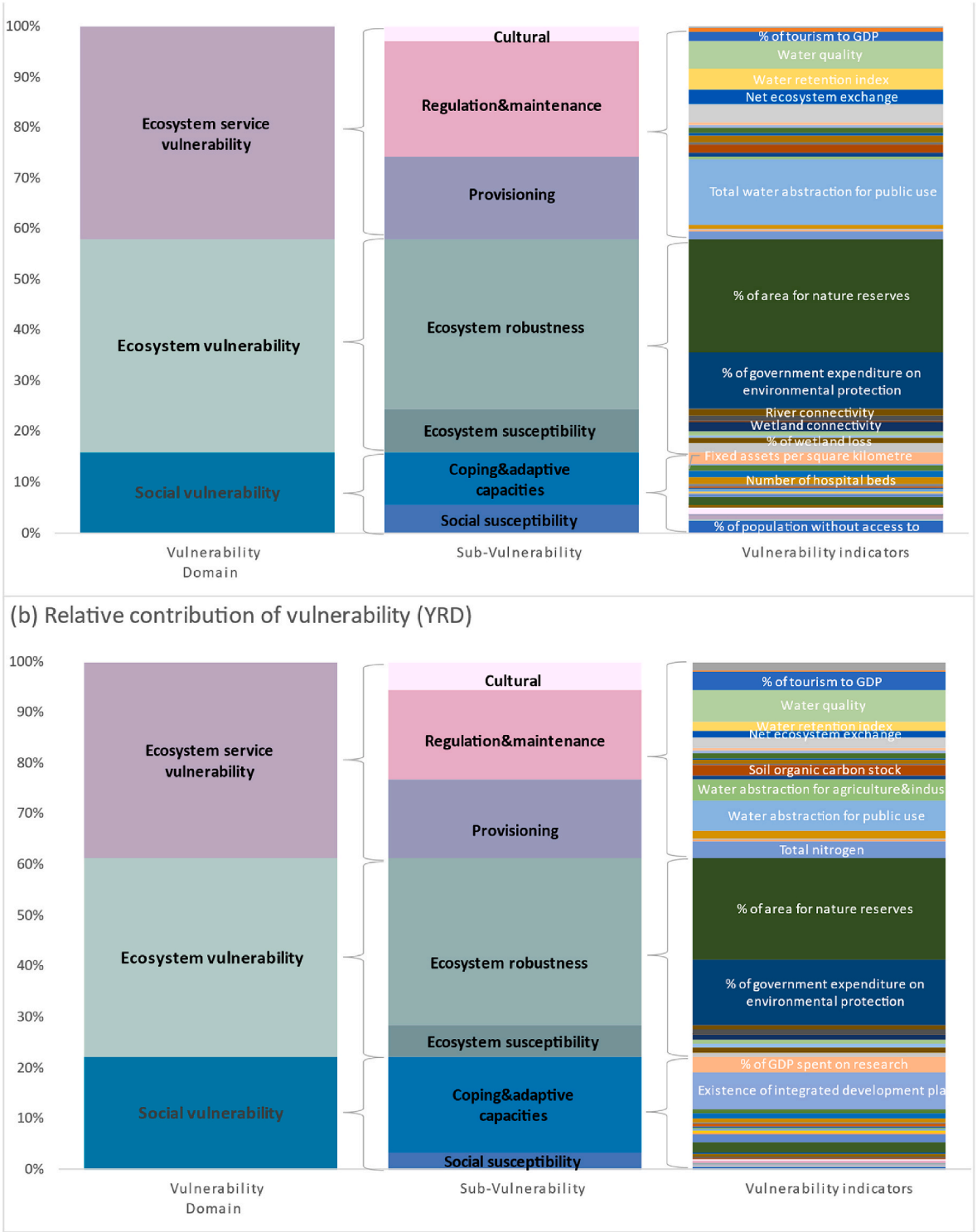


**Fig. 8.** (a) and (b): Relative contributions of the vulnerability domains, sub-vulnerability components and vulnerability indicators to the final vulnerability score in the PRD and YRD.

sub-vulnerability components and indicators that have relatively high contributions to the final vulnerability score. Key drivers of social vulnerability in both deltas include indicators of no access to clean water, public health expenditure and funding for scientific research and development. Deforested areas and low river connectivity in the PRD and wetland loss in the YRD are important drivers of ecosystem susceptibility. Besides, vegetation greenness (NDVI) has a high influence on ecosystem susceptibility in the two deltas. Low coverage of nature reserves and insufficient government expenditure on environmental protection, which belong to ecosystem robustness, are both critical factors for the final vulnerability scores. The relatively high contribution of these two indicators is also related to being assigned high weights of 11.8% and 10.7%. The vulnerability distribution in the two deltas is mainly driven by ecosystem services and ecosystem vulnerability, with social vulnerability, though assigned a weight of 33%, making a relatively low contribution (PRD: 16%, YRD: 22%).

Regulation & maintenance services in the vulnerability of ecosystem services include important drivers, especially in soil quality, erosion control, climate, water and biodiversity. Water regulation (water retention index and water quality index) is the most critical factor affecting each delta's ecosystem services and final vulnerability. In terms of provisioning services, agriculture production (biomass) and water abstraction for public use (water sources) are the important drivers in the two deltas. Total water abstraction for agriculture and industry use (water sources provisioning) in YRD also contributes significantly to the final vulnerability score. Additionally, percentage of tourism to GDP is an important driver of cultural services in PRD and YRD. The ecological vulnerability (ecosystem service and ecosystem vulnerability) contributed 84% (ecosystem services accounted for 42%) in PRD and 78% (ecosystem services accounted for 39%) in YRD. This information can help develop targeted risk policies from the perspective of environmental strategies.

## 4. Discussion and outlook

### 4.1. Mapping risks to identify priority issues

Indicator-based risk assessment combined with GIS has proven to be an informative tool for assessing spatial risk distribution and helping management at all levels to take appropriate actions to reduce risks. There are two main categories of contributions from this research. One is to the existing risk assessment research, the proposed Delta-ES-SES framework with modular indicator list method has several advantages: (1) It allows collecting a large number of different data, and regularly updating the original data to obtain new risk scores. Risk scores can be easily analysed spatially, allowing managers to capture information at different scales; (2) This framework can adjust indicators and weights according to the specific situation or development goals of each region and can incorporate new hazard types and indicators; (3) Integrating the concept of ecosystem services into the vulnerability domain allows capturing the health status of ecosystems, but also facilitate identifying the corresponding contribution of ecosystem service to vulnerability and risk. Furthermore, incorporating customized ecosystem service-based protection measures into risk management and reduction ensures that ecosystems sustainably deliver services to human and social systems; (4) A detailed and subdivided multi-level indicator library allows scientists and experts to connect hazards with vulnerability and risk concepts, and be more capable of taking risk-informed decisions.

The other contribution is to the wider community, as our results clarified the risk levels of the two studied deltas. Risk assessments at the delta and city level primarily serve to identify areas with higher incidences of natural hazards, higher levels of economics/population/ecosystem exposure, vulnerability and risks in the study sites (such as Zhongshan in PRD and Taizhou_J in YRD), which constitutes the key prerequisites for developing effective risk reduction strategies. The final risk distribution aligns with findings in other studies concerning the risk of the YRD, where the southeastern region consistently exhibits high-risk distribution (Bai et al., 2023; Ou et al., 2022). As areas prone to natural hazards are likely to experience more recurring and intense extreme events in the future (Schwarz and Kuleshov, 2022), there is a need for more precise risk assessments at small spatial scales (urban--rural or village level). This process can better incorporate local knowledge and at the same time improve local understanding of risks at different levels. Collaboration, preparation and mitigation solutions across sectors and scales help advance risk assessments (Quesada-Román and Campos-Durán, 2023).

The analysis shows that the magnitude of risk in an area does not always match the underlying vulnerability, with situations of low vulnerability-high risk and high hazard exposure-low risk. This type of information can be used as supporting evidence for the potential effectiveness of existing decision-making with respect to risk reduction measures. For example, the high-risk but low-vulnerability tract of Yancheng in the YRD could suggest there might be certain useful risk prevention and control measures to reduce vulnerability that have been implemented in areas highly exposed to multiple hazards. High values in frequency, intensity, exposure and vulnerability have jointly led to high-risk levels, including in Zhongshan and Foshan in the PRD, and in the Yangzhou and Taizhou_J in YRD, which urgently need attention. Comparative studies have shown that even though study areas both belong to coastal river deltas, they face different major natural hazards. Breaking down multiple hazard components shows that the PRD faces a high intensity of cyclones and storm surges, while the YRD is more exposed to drought. These findings are in line with two separate assessments of typhoon risk in China, with the PRD identified as the significant risk hotspot, followed by Zhejiang Province in the YRD (Sajjad et al., 2020; Yin et al., 2013). While not reflected in the calculated risk index, we acknowledge the significance of other hazards in the delta regions, such as Harmful Algal Blooms (toxic red tide in the study area) mentioned during the expert consultation, with official reports confirming its occurrence in Shenzhen of PRD and several areas of YRD (DNR, 2020).

The distribution of exposed population and economic values, denoting social exposure, typically exhibits consistent trends. The definition of ecosystems does not encompass artificial surfaces, potentially leading to disparities in spatial distribution between ecosystem exposure and social exposure. In densely developed areas, such as the majority of the PRD, social exposure levels are higher than ecosystem exposure. Through an examination of the spatial profiles in risk, hazard * exposure, and vulnerability, we noted a convergence of multi-hazard risk and hazard exposure scores, implying that the disparities in risk are noticeably associated with hazard magnitude and extent. The future trends in risks are significantly impacted by the variability and distribution of hazard events, highlighting the key to monitoring these, especially at the regional level (Tessler et al., 2015). Using advanced machine learning models to simulate, monitor and predict hazardous events has been proven effective in hazard description and risk assessments (Abu El-Magd et al., 2022; Antzoulatos et al., 2022; Mallick et al., 2021; Pourghasemi et al., 2021; Towfiqul Islam et al., 2021; Wang et al., 2015). These techniques deserve further exploration, such as exploring the impact of cascading hazards to enhance future risk mitigation and reduction measures (Komendantova et al., 2014).

### 4.2. Policy implications of vulnerability component

Priority 1 of the Sendai Framework for Disaster Risk Reduction 2015–2030 underscores the need to comprehensively grasp all dimensions of risk, encompassing vulnerability and the environment, to inform effective risk management (UNDRR, 2015). It is important to assess their social and ecological vulnerability to better minimize damage to social systems or ecosystems. The effects of vulnerability indicators in risk assessments are not equal in all cities, and they affect trends in each vulnerability sub-component differently. Multiple social

sectors are exposed to natural hazards, especially the urban areas are highly vulnerable to multiple hazards due to population concentration and infrastructure density (Jones et al., 2015). For social susceptibility, the indicators 'percentage of population without access to clean water' and 'percentage malnourished population' of PRD and 'percentage of families below the poverty line in total households' of YRD are the main influencing factors. In addition to the common key driver of 'GDP per capita', the indicators 'number of hospital beds per 1000 inhabitants' and 'public health expenditure' were found to be the driving factors affecting the coping capacity of the PRD. This means that the improvement of the medical system is an angle worthy of attention in future risk response in the PRD. Meanwhile, environmental protection policies and scientific research funding would have a relatively large impact on the adaptive capacity when facing risks. This study further highlights the key drivers such as forest and wetland loss for ecosystem health, consistent with risk assessment in the Mississippi Delta (Anderson et al., 2021).

Systematically incorporating ecosystem services into the vulnerability domain enables a more integrated understanding of the health of ecosystems and their ability to provide services that are directly or indirectly linked to vulnerability components. Ecosystem services capture the intricate interactions between humans and nature, and serve as a common link between social and ecosystem vulnerability. It is an opportunity to understand better the environmental dimension of risk profiles. Meanwhile, ecosystem services are also closely related to concepts such as ecosystem-based adaptation (EbA), nature-based solutions (NBS) and ecosystem-based disaster risk reduction (Eco-DRR) (IPCC, 2022; Shah et al., 2023), which have been increasingly accepted to help people adapt to adverse effects of climate change (Seddon et al., 2020) and to reduce risks from natural hazards (Shah et al., 2020). As mentioned before, the key role of water sources (provisioning service) and water quality (regulation & maintenance) reflects the high dependence of delta development on ecosystem services, especially in the Anhui Province (inland of YRD). It connects risk management to water resource management and water policy related to the restoration of aquatic ecosystems (Grizzetti et al., 2016). Conducting vulnerability assessments from biophysical (water quality) and economic (water abstraction) highlights the interdependence of humans and ecosystems. Likewise, agricultural productivity is the key human activity in both deltas, not only directly related to human well-being but also reflecting the need for risk management in areas highly dependent on agriculture (or other biomass productivity). This could inspire a range of ecosystem-based sustainable conservation practices in agroforests and farmland, which also maintain and improve ecosystem services such as food provision, soil nutrient regulation and climate regulation (Blaser et al., 2018). Cultural context is also an aspect of vulnerability, and it includes valuable cultural components such as heritage and tourist attractions. The number of nature reserves and the development of tourism are important for understanding the stability of ecosystems. All of these introduce the method of assessing SES with the role of ecosystem services to sustainably manage, protect and prevent damage to ecosystems and their services (De Lange et al., 2010). Even in hazard-prone regions, better SES health can be achieved in long-term and sustainable ways by conserving natural resources and landscapes.

### 4.3. Limitations and way forward

To the best of our knowledge, our study is the first to conduct comparative SES-based risk assessments in the YRD and PRD regions and with a framework that incorporates the role of ecosystem services. Identifying areas with high-risk levels in these two most prosperous, densely populated, and hazard-prone areas is an effective way to reduce the negative impact of multiple natural hazards. Its application has certain limitations, such as the uncertainty brought by the use of expert weights (Gonzalez-Ollauri et al., 2023). In order to address this issue, we compared and analysed different risk profiles with expert weights and equal weights, and found that there were no obvious differences in risk scores. Nonetheless, the influence of expert-assigned weights on the relative contribution of vulnerability subcomponents and their respective indicators is an unavoidable factor. The accuracy of the data also needs to be continuously improved. It should be noted that the risk assessment relies on differences in various components across regions. In this study, we made maximum use of available spatial data as well as existing data appropriate to the study area. However, some data on vulnerability indicators were not available for small administrative regions, so we had to use average provincial data and profile the risk map at the city-level. We deem this has only a minimal impact on the final risk score, as provincial units can illustrate differences in development and management levels for the Yangtze and Pearl River Deltas. Because of this, we cannot directly capture the distinction between urban and rural areas, yet key drivers of vulnerability may differ in rural and urban areas (Kc et al., 2021). Due to the distribution of diverse ecosystem types, significant differences may exist in the supply of ecosystem services between urban and rural areas. We, therefore, emphasize the necessity for future research to zoom in on the selected cities in the deltas to the county level to capture urban-rural differences for the development of more targeted regional policy and action plans.

Despite the emphasis on the progress of SES theory, the practices still bring inherent limitations, that is, it is difficult to identify specific coupling dynamics and other synergies (Anderson et al., 2021). We added the ecosystem services perspective and expert judgments to address this and better characterize the vulnerability and risk distribution. Various ecosystems offer different primary ecosystem services; for instance, mangroves contribute to biodiversity preservation and mitigating the adverse effects of coastal natural hazards, and their restoration is widely recognized as an ecosystem-based adaptation approach (Chausson et al., 2020). This also further emphasizes the data availability of ecosystem service indicators, especially for specific ecosystem types, which can be combined with high-resolution spatial data sets and local residents' perceptions of various services. Moreover, although static and spatially explicit approaches are highly realistic models, they fail to take into account interactions between adjacent areas, which is the inevitable compromise between complexity and practicality to represent reality in risk assessment (Anderson et al., 2021).

Quantifying stakeholder values of ecosystem services (requiring downscaled research) or system modelling (technically complex) in an SES vulnerability context at delta scales poses challenges. Therefore, we adopted an interdisciplinary approach to build on existing ecosystem service classifications and related research results, using this information to develop indicators which allowed us to compute indices. Our analysis of ecosystem services also reflects trade-offs in reducing complexity which brings its own limitations. What is needed in future research is small-scale studies with high-resolution spatial data and local stakeholders' involvement to facilitate more reliable assessment and comparison of spatially distributed risks. The application of proxy indicators also causes uncertainty, which calls on management departments at all levels to pay attention to data collection and management (Hagenlocher et al., 2018), and can further improve and supplement the indicators selected for risk dimensions in subsequent research. Additionally, the uncertainty after the COVID-19 pandemic is not considered, which affects the development of social-ecological systems, especially socio-economic activities.

This study will serve as the basis for further analysis of the deltaic multi-hazard risk index by incorporating ecosystem service indicators in the vulnerability domain. This aims to make the adjustable risk indicators and data in this study accessible to stakeholders in the study area and linked to ecosystem conservation measures or the deployment of nature-based solutions that can be implemented. In fact, this comprehensive framework and list of indicators can be replicated and adapted worldwide and is relatively easy to use. In the future, we can continue to explore the internal differences and develop a framework of ecosystem-based adaptation measures.

## 5. Conclusion

This paper applied an improved vulnerability and risk assessment framework for deltaic environments, mainly composed of applicable and easily accessible indicators. Vulnerability is quantified with indicators linking ecosystem services-based management measures and has been applied to the PRD and YRD. It also makes progress towards capturing the muti-hazard risk characteristics of all cities in the PRD and YRD regions exposed to five natural hazards (i.e. floods, typhoons, storm surges, droughts and salt intrusion). In addition to multi-hazard risk, a single-hazard risk profile is available for each region. Visualization maps allow users to readily compare and interpret the data distribution of each area for different risk attributes (hazard, exposure, and vulnerability). The risk index also allows looking at specific components and their indicators with high contribution to risk, some examples have already been given. Given the current divergence in spatial patterns of hazard exposure and social and ecological vulnerability within both deltas, future risk reduction planning should account for sub-component characteristics as well as individual/combined hazard impacts.

The importance of the proposed risk framework is that it directly and systematically incorporates ecosystem services and achieves the balance of social and ecological dimensions. It improved a lot on clarifying (multi-)hazard risk components and provided an integrated view for risk assessments of social-ecological systems. While previous work can also discern key risk indicators, the proposed methodology can explicitly extract ecosystem service indicators that affect human well-being, and which can be optimally used to inform current risk reduction and nature-based solutions practices.

## Ethics statement

This study was approved by the Research Ethics Committee, College of Social Sciences, University of Glasgow, UK and follows the General Data Protection Regulation (GDPR). The participants provided their signed consent forms.

## CRediT authorship contribution statement

**Yuting Peng:** Conceptualization, Data curation, Methodology, Software, Visualization, Writing – original draft, Writing – review & editing. **Natalie Welden:** Conceptualization, Methodology, Supervision, Writing – review & editing. **Fabrice G. Renaud:** Conceptualization, Methodology, Supervision, Writing – review & editing.

## Declaration of competing interest

The authors declare that they have no known competing financial interests or personal relationships that could have appeared to influence the work reported in this paper.

## Data availability

We have shared the link to our data sources in Supplementary Material.

## Acknowledgements

We would like to thank (i) all experts for their valuable feedback regarding indicator selection and weight distribution, (ii) Michelle van Vliet and Keke Zhou for sharing data.

## Appendix A. Supplementary data

Supplementary data to this article can be found online at https://doi.org/10.1016/j.ocecoaman.2023.106980.

## References

Abu El-Magd, S.A., Maged, A., Farhat, H.I., 2022. Hybrid-based Bayesian algorithm and hydrologic indices for flash flood vulnerability assessment in coastal regions: machine learning, risk prediction, and environmental impact. Environ. Sci. Pollut. Res. 29 https://doi.org/10.1007/s11356-022-19903-7.

Anderson, C.C., Renaud, F.G., Hagenlocher, M., Day, J.W., 2021. Assessing multi-hazard vulnerability and dynamic coastal flood risk in the Mississippi delta: the global delta risk index as a social-ecological systems approach. Water (Basel) 13. https://doi.org/10.3390/w13040577.

Anelli, D., Tajani, F., Ranieri, R., 2022. Urban resilience against natural disasters: mapping the risk with an innovative indicators-based assessment approach. J. Clean. Prod. 371, 133496 https://doi.org/10.1016/J.JCLEPRO.2022.133496.

Anthony, E.J., 2015. Deltas. In: Masselink, G., Gehrels, R. (Eds.), Coastal Environments and Global Change. John Wiley & Sons, Ltd, Chichester, UK, pp. 299–337. https://doi.org/10.1002/9781119117261.ch13.

Antzoulatos, G., Kouloglou, I.O., Bakratsas, M., Moumtzidou, A., Gialampoukidis, I., Karakostas, A., Lombardo, F., Fiorin, R., Norbiato, D., Ferri, M., Symeonidis, A., Vrochidis, S., Kompatsiaris, I., 2022. Flood hazard and risk mapping by applying an explainable machine learning framework using satellite imagery and GIS data. Sustainability 14. https://doi.org/10.3390/su14063251.

Armatas, C., Venn, T., Watson, A., 2017. Understanding social–ecological vulnerability with Q-methodology: a case study of water-based ecosystem services in Wyoming, USA. Sustain. Sci. 12, 105–121.

Bai, J., Guo, K., Liu, M., Jiang, T., 2023. Spatial variability, evolution, and agglomeration of eco-environmental risks in the Yangtze River Economic Belt, China. Ecol. Indicat. 152, 110375 https://doi.org/10.1016/j.ecolind.2023.110375.

Berrouet, L., Villegas-Palacio, C., Botero, V., 2019. A social vulnerability index to changes in ecosystem services provision at local scale: a methodological approach. Environ. Sci. Pol. 93, 158–171. https://doi.org/10.1016/j.envsci.2018.12.011.

Blaser, W.J., Oppong, J., Hart, S.P., Landolt, J., Yeboah, E., Six, J., 2018. juneClimate-smart sustainable agriculture in low-to-intermediate shade agroforests. Nat. Sustain. 1, 234–239. https://doi.org/10.1038/s41893-018-0062-8.

Brondizio, E.S., Foufoula-Georgiou, E., Szabo, S., Vogt, N., Sebesvari, Z., Renaud, F.G., Newton, A., Anthony, E., Mansur, A.V., Matthews, Z., Hetrick, S., Costa, S.M., Tessler, Z., Tejedor, A., Longjas, A., Dearing, J.A., 2016a. Catalyzing action towards the sustainability of deltas. Curr. Opin. Environ. Sustain. 19, 182–194. https://doi.org/10.1016/j.cosust.2016.05.001.

Brondizio, E.S., Vogt, N.D., Mansur, A.V., Anthony, E.J., Costa, S., Hetrick, S., 2016b. A conceptual framework for analyzing deltas as coupled social–ecological systems: an example from the Amazon River Delta. Sustain. Sci. 11, 591–609. https://doi.org/10.1007/s11625-016-0368-2.

Chang, H., Pallathadka, A., Sauer, J., Grimm, N.B., Zimmerman, R., Cheng, C., Iwaniec, D.M., Kim, Y., Lloyd, R., McPhearson, T., Rosenzweig, B., Troxler, T., Welty, C., Brenner, R., Herreros-Cantis, P., 2021. Assessment of urban flood vulnerability using the social-ecological-technological systems framework in six US cities. Sustain. Cities Soc. 68, 102786 https://doi.org/10.1016/j.scs.2021.102786.

Chausson, A., Turner, B., Seddon, D., Chabaneix, N., Girardin, C.A.J., Kapos, V., Key, I., Roe, D., Smith, A., Woroniecki, S., Seddon, N., 2020. Mapping the effectiveness of nature-based solutions for climate change adaptation. Global Change Biol. 26, 6134–6155. https://doi.org/10.1111/gcb.15310.

Chen, Y., Li, J., Chen, A., 2021. Does high risk mean high loss: evidence from flood disaster in southern China. Sci. Total Environ. 785, 147127 https://doi.org/10.1016/j.scitotenv.2021.147127.

Chen, Y.D., Zhang, Q., Xiao, M., Singh, V.P., Zhang, S., 2016. Probabilistic forecasting of seasonal droughts in the Pearl River basin, China. Stoch. Environ. Res. Risk Assess. 30, 2031–2040. https://doi.org/10.1007/s00477-015-1174-6.

CMA, 2014. The Tropical Cyclone Yearbook. Beijing.

Collins, S.L., Carpenter, S.R., Swinton, S.M., Orenstein, D.E., Childers, D.L., Gragson, T. L., Grimm, N.B., Grove, J.M., Harlan, S.L., Kaye, J.P., Knapp, A.K., Kofinas, G.P., Magnuson, J.J., McDowell, W.H., Melack, J.M., Ogden, L.A., Robertson, G.P., Smith, M.D., Whitmer, A.C., 2011. An integrated conceptual framework for long-term social–ecological research. Front. Ecol. Environ. 9, 351–357. https://doi.org/10.1890/100068.

CRED, UNDRR, 2020. The Human Cost of Disasters: an Overview of the Last 20 Years (2000-2019), Human Cost of Disasters.

Cremin, E., O'Connor, J., Banerjee, S., Bui, L.H., Chanda, A., Hua, H.H., Van Huynh, D., Le, H., Murshed, S.B., Mashfiqus, S., Vu, A., Sebesvari, Z., Large, A., Renaud, F.G., 2023. Aligning the Global Delta Risk Index with SDG and SFDRR global frameworks to assess risk to socio-ecological systems in river deltas. Sustain. Sci. 18, 1871–1891. https://doi.org/10.1007/s11625-023-01295-3.

Cutter, S.L., Boruff, B.J., Shirley, W.L., 2003. Social vulnerability to environmental hazards. Soc. Sci. Q. 84, 242–261. https://doi.org/10.1111/1540-6237.8402002.

Dalrymple, R.W., Choi, K., 2007. Morphologic and facies trends through the fluvial–marine transition in tide-dominated depositional systems: a schematic framework for environmental and sequence-stratigraphic interpretation. Earth Sci. Rev. 81, 135–174. https://doi.org/10.1016/J.EARSCIREV.2006.10.002.

De Lange, H.J., Sala, S., Vighi, M., Faber, J.H., 2010. Ecological vulnerability in risk assessment — a review and perspectives. Sci. Total Environ. 408, 3871–3879. https://doi.org/10.1016/j.scitotenv.2009.11.009.

Depietri, Y., 2020. The social–ecological dimension of vulnerability and risk to natural hazards. Sustain. Sci. 15, 587–604. https://doi.org/10.1007/s11625-019-00710-y.

Dewan, A.M., 2013. Hazards, risk, and vulnerability. In: Dewan, A. (Ed.), Floods in a Megacity. Springer Netherlands, Dordrecht, pp. 35–74. https://doi.org/10.1007/978-94-007-5875-9_2.

DNR, 2020. Zhejiang Marine Disaster Bulletin.

Fang, J., Lincke, D., Brown, S., Nicholls, R.J., Wolff, C., Merkens, J.-L., Hinkel, J., Vafeidis, A.T., Shi, P., Liu, M., 2020. Coastal flood risks in China through the 21st century – an application of DIVA. Sci. Total Environ. 704, 135311 https://doi.org/10.1016/j.scitotenv.2019.135311.

Fengwei, L., Kwang, P.K., Xiuli, D., Mingju, Z., 2013. Improved AHP method and its application in risk identification. J. Construct. Eng. Manag. 139, 312–320. https://doi.org/10.1061/(ASCE)CO.1943-7862.0000605.

Francesco, D., Peter, S., Lorenzo, A., Alessandra, B., Luc, F., Feyera, H., Valerio, L., 2016. Flood hazard maps at European and global scale [WWW Document]. European Commission, Joint Research Centre. URL. https://data.jrc.ec.europa.eu/collection/id-0054.

GADM, 2018. GADM Maps. Version 3.6 [WWW Document]. URL. https://gadm.org/index.html.

Gallina, V., Torresan, S., Critto, A., Sperotto, A., Glade, T., Marcomini, A., 2016. A review of multi-risk methodologies for natural hazards: consequences and challenges for a climate change impact assessment. J. Environ. Manag. 168, 123–132. https://doi.org/10.1016/j.jenvman.2015.11.011.

Ge, Y., Dou, W., Dai, J., 2017. A new approach to identify social vulnerability to climate change in the Yangtze River Delta. Sustainability 9, 2236. https://doi.org/10.3390/su9122236.

Ge, Y., Dou, W., Gu, Z., Qian, X., Wang, J., Xu, W., Shi, P., Ming, X., Zhou, X., Chen, Y., 2013. Assessment of social vulnerability to natural hazards in the Yangtze River Delta, China. Stoch Env Res Risk A27, 1899–1908. https://doi.org/10.1007/s00477-013-0725-y.

Giosan, L., Syvitski, J., Constantinescu, S., Day, J., 2014. Climate change: protect the world's deltas. Nature. https://doi.org/10.1038/516031a.

Gonzalez-Ollauri, A., Mickovski, S.B., Anderson, C.C., Debele, S., Emmanuel, R., Kumar, P., Loupis, M., Ommer, J., Pfeiffer, J., Panga, D., Pilla, F., Sannigrahi, S., Toth, E., Ukonmaanaho, L., Zieher, T., 2023. A nature-based solution selection framework: criteria and processes for addressing hydro-meteorological hazards at open-air laboratories across Europe. J. Environ. Manag. 331, 117183 https://doi.org/10.1016/j.jenvman.2022.117183.

Gracia, A., Rangel-Buitrago, N., Oakley, J.A., Williams, A.T., 2018. Use of ecosystems in coastal erosion management. Ocean Coast Manag. 156, 277–289. https://doi.org/10.1016/j.ocecoaman.2017.07.009.

Grizzetti, B., Lanzanova, D., Liquete, C., Reynaud, A., Cardoso, A.C., 2016. Assessing water ecosystem services for water resource management. Environ. Sci. Pol. 61, 194–203. https://doi.org/10.1016/j.envsci.2016.04.008.

Hagenlocher, M., Meza, I., Anderson, C.C., Min, A., Renaud, F.G., Walz, Y., Siebert, S., Sebesvari, Z., 2019. Drought vulnerability and risk assessments: state of the art, persistent gaps, and research agenda. Environ. Res. Lett. 14, 083002 https://doi.org/10.1088/1748-9326/ab225d.

Hagenlocher, M., Renaud, F.G., Haas, S., Sebesvari, Z., 2018. Vulnerability and risk of deltaic social-ecological systems exposed to multiple hazards. Sci. Total Environ. 631–632, 71–80. https://doi.org/10.1016/J.SCITOTENV.2018.03.013.

Haines-Young, R., Potschin, M., 2018. Common International Clasification of Ecosystem Services CICES V5. 1. Guidance on the Application of the Revised Structure [WWW Document]. URL. www.cices.eu.

Hoitink, A.J.F., Nittrouer, J.A., Passalacqua, P., Shaw, J.B., Langendoen, E.J., Huismans, Y., van Maren, D.S., 2020. Resilience of River Deltas in the anthropocene. J Geophys Res Earth Surf 125. https://doi.org/10.1029/2019JF005201.

IFRC, 2022. What are hazards? [WWW Document]. URL. https://www.ifrc.org/what-disaster.

IPCC, 2022. Climate Change 2022: Impacts, Adaptation and Vulnerability. https://doi.org/10.1017/9781009325844. Cambridge, UK and New York, NY, USA.

Ishizaka, A., Labib, A., 2011. Review of the main developments in the analytic hierarchy process. Expert Syst. Appl. 38 https://doi.org/10.1016/j.eswa.2011.04.143.

Jian, W., Li, S., Lai, C., Wang, Z., Cheng, X., Lo, E.Y.-M., Pan, T.-C., 2021. Evaluating pluvial flood hazard for highly urbanised cities: a case study of the Pearl River Delta Region in China. Nat. Hazards 105, 1691–1719. https://doi.org/10.1007/s11069-020-04372-3.

Jones, B., O'Neill, B.C., McDaniel, L., McGinnis, S., Mearns, L.O., Tebaldi, C., 2015. Future population exposure to US heat extremes. Nat. Clim. Change 5, 652–655. https://doi.org/10.1038/nclimate2631.

Kc, B., Shepherd, J.M., King, A.W., Johnson Gaither, C., 2021. Multi-hazard climate risk projections for the United States. Nat. Hazards 105. https://doi.org/10.1007/s11069-020-04385-y.

Kirby, R.H., Reams, M.A., Lam, N.S.N., Zou, L., Dekker, G.G.J., Fundter, D.Q.P., 2019. Assessing social vulnerability to flood hazards in the Dutch province of zeeland. Int J Disast Risk Sc 10, 233–243. https://doi.org/10.1007/s13753-019-0222-0.

Komendantova, N., Mrzyglocki, R., Mignan, A., Khazai, B., Wenzel, F., Patt, A., Fleming, K., 2014. Multi-hazard and multi-risk decision-support tools as a part of participatory risk governance: feedback from civil protection stakeholders. Int. J. Disaster Risk Reduc. 8, 50–67. https://doi.org/10.1016/j.ijdrr.2013.12.006.

Kundzewicz, Z., Su, B., Wang, Y., Xia, J., Huang, J., Jiang, T., 2019. Flood risk and its reduction in China. Adv. Water Resour. 130, 37–45. https://doi.org/10.1016/j.advwatres.2019.05.020.

Li, K., Li, G.S., 2011. Vulnerability assessment of storm surges in the coastal area of Guangdong Province. Nat Hazard Earth Sys 11, 2003–2010. https://doi.org/10.5194/nhess-11-2003-2011.

Liang, C., Mo, X.-J., Xie, J.-F., Wei, G.-L., Liu, L.-Y., 2022. Organophosphate tri-esters and di-esters in drinking water and surface water from the Pearl River Delta, South China: implications for human exposure. Enviro Pollut 313, 120150. https://doi.org/10.1016/j.envpol.2022.120150.

Lilai, X., Yuanrong, H., Wei, H., shenghui, C., 2016. A multi-dimensional integrated approach to assess flood risks on a coastal city, induced by sea-level rise and storm tides. Environ. Res. Lett. 11, 014001 https://doi.org/10.1088/1748-9326/11/1/014001.

Lin, W., Sun, Y., Nijhuis, S., Wang, Z., 2020. Scenario-based flood risk assessment for urbanizing deltas using future land-use simulation (FLUS): guangzhou Metropolitan Area as a case study. Sci. Total Environ. 739, 139899 https://doi.org/10.1016/j.scitotenv.2020.139899.

Liu, B., Siu, Y.L., Mitchell, G., Xu, W., 2013. Exceedance probability of multiple natural hazards: risk assessment in China's Yangtze River Delta. Nat. Hazards 69, 2039–2055. https://doi.org/10.1007/s11069-013-0794-8.

Lozoya, J., Conde, D., Asmus, M., Polette, M., Píriz, C., Martins, F., de Álava, D., Marenzi, R., Nin, M., Anello, L., 2015. Linking Social Perception and Risk Analysis to Assess Vulnerability of Coastal Socio-Ecological Systems to Climate Change in Atlantic South America. Handbook of Climate Change Adaptation. Springer, Berlin, Germany, pp. 373–399.

Mallick, J., Alqadhi, S., Talukdar, S., Alsubih, M., Ahmed, M., Khan, R.A., Kahla, N. Ben, Abutayeh, S.M., 2021. Risk assessment of resources exposed to rainfall induced landslide with the development of gis and rs based ensemble metaheuristic machine learning algorithms. Sustainability 13. https://doi.org/10.3390/su13020457.

Marin-Ferrer, M., Vernaccini, L., Poljansek, K., 2017. INFORM Index for Risk Management. European Commission.

MNR, 2021. Bulletin of China Marine Disaster 2020 [WWW Document]. URL. http://www.mnr.gov.cn/sj/sjfw/hy/gbgg/zghyzhgb/. accessed 4.18.22.

Morelli, A., Taramelli, A., Bozzeda, F., Valentini, E., Colangelo, M.A., Cueto, Y.R., 2021. The disaster resilience assessment of coastal areas: a method for improving the stakeholders' participation. Ocean Coast Manag. 214, 105867 https://doi.org/10.1016/j.ocecoaman.2021.105867.

Muis, S., Verlaan, M., Winsemius, H.C., Aerts, J.C.J.H., Ward, P.J., 2016. A global reanalysis of storm surges and extreme sea levels. Nat. Commun. 7, 11969 https://doi.org/10.1038/ncomms11969.

Nardo, M., Saisana, M., Saltelli, A., Tarantola, S., 2005. Tools for composite indicators building. European Comission, Ispra 15, 19–20.

CCCS, 2021. ERA5 (1979-2020) [WWW Document]. ECMWF. https://www.ecmwf.int/en/forecasts/datasets/reanalysis-datasets/era5%0D%0A.

NBS, 2004. China National Conditions and Strength. Beijing.

NBS, 2020. China Statistical Yearbook 2020. Beijing.

Ng, K., Borges, P., Phillips, M.R., Medeiros, A., Calado, H., 2019. An integrated coastal vulnerability approach to small islands: the Azores case. Sci. Total Environ. 690 https://doi.org/10.1016/j.scitotenv.2019.07.013.

NGCC, 2020. Land Cover Map (GlobeLand 30 - NGCC) [WWW Document]. URL http://www.globallandcover.com/home_en.html.

Nhamo, L., Ndlela, B., Nhemachena, C., Mabhaudhi, T., Mpandeli, S., Matchaya, G., 2018. The water-energy-food nexus: climate risks and opportunities in Southern Africa. Water (Switzerland). https://doi.org/10.3390/w10050567.

Nicholls, R.J., Cazenave, A., 2010. Sea-level rise and its impact on coastal zones. Science 1979. https://doi.org/10.1126/science.1185782.

Ou, X., Lyu, Y., Liu, Y., Zheng, X., Li, F., 2022. Integrated multi-hazard risk to social-ecological systems with green infrastructure prioritization: a case study of the Yangtze River Delta, China. Ecol. Indicat. 136, 108639 https://doi.org/10.1016/j.ecolind.2022.108639.

Ouma, Y., Tateishi, R., 2014. Urban flood vulnerability and risk mapping using integrated multi-parametric AHP and GIS: methodological overview and case study assessment. Water (Basel) 6, 1515–1545. https://doi.org/10.3390/w6061515.

Pathan, A.I., Girish Agnihotri, P., Said, S., Patel, D., 2022. AHP and TOPSIS based flood risk assessment- a case study of the Navsari City, Gujarat, India. Environ. Monit. Assess. 194, 509. https://doi.org/10.1007/s10661-022-10111-x.

Peduzzi, P., 2014. Global Risk Data Platform - Cyclone [WWW Document]. UNEP/DEWA/GRID-Europe. URL. https://preview.grid.unep.ch/index.php?preview=data&events=cyclones&evcat=1&lang=eng. accessed 4.16.22.

Peng, Y., Welden, N., Renaud, F.G., 2023. A framework for integrating ecosystem services indicators into vulnerability and risk assessments of deltaic social-ecological systems. J. Environ. Manag. 326, 116682 https://doi.org/10.1016/j.jenvman.2022.116682.

Pourghasemi, H.R., Amiri, M., Edalat, M., Ahrari, A.H., Panahi, M., Sadhasivam, N., Lee, S., 2021. Assessment of urban infrastructures exposed to flood using susceptibility map and google earth engine. IEEE J. Sel. Top. Appl. Earth Obs. Rem. Sens. 14 https://doi.org/10.1109/JSTARS.2020.3045278.

PSB, 2019. Guangdong Statistical Yearbook (2019). Guangzhou.

Quesada-Román, A., Campos-Durán, D., 2023. Natural disaster risk inequalities in Central America. Pap Appl Geogr 9, 36–48. https://doi.org/10.1080/23754931.2022.2081814.

Rangel-Buitrago, N., Neal, W.J., de Jonge, V.N., 2020. Risk assessment as tool for coastal erosion management. Ocean Coast Manag. 186, 105099 https://doi.org/10.1016/j.ocecoaman.2020.105099.

Saaty, T.L., 2008. Decision making with the analytic hierarchy process. Int. J. Serv. Sci. 1, 83–98. https://doi.org/10.1504/IJSSCI.2008.017590.

Sajjad, M., Chan, J.C.L., Kanwal, S., 2020. Integrating spatial statistics tools for coastal risk management: a case-study of typhoon risk in mainland China. Ocean Coast Manag. 184, 105018 https://doi.org/10.1016/j.ocecoaman.2019.105018.

Saura, S., Torné, J., 2009. Conefor Sensinode 2.2: a Software Package for Quantifying the Importance of Habitat Patches for Landscape Connectivity.

Schwarz, I., Kuleshov, Y., 2022. Flood vulnerability assessment and mapping: a case study for Australia's hawkesbury-nepean catchment. Rem. Sens. 14 https://doi.org/10.3390/rs14194894.

Sebesvari, Z., Renaud, F.G., Haas, S., Tessler, Z., Hagenlocher, M., Kloos, J., Szabo, S., Tejedor, A., Kuenzer, C., 2016. A review of vulnerability indicators for deltaic

social–ecological systems. Sustain. Sci. 11, 575–590. https://doi.org/10.1007/s11625-016-0366-4.
Seddon, N., Daniels, E., Davis, R., Chausson, A., Harris, R., Hou-Jones, X., Huq, S., Kapos, V., Mace, G.M., Rizvi, A.R., Reid, H., Roe, D., Turner, B., Wicander, S., 2020. Global recognition of the importance of nature-based solutions to the impacts of climate change. Global Sustainability 3, e15. https://doi.org/10.1017/sus.2020.8.
Shah, M.A.R., Renaud, F.G., Anderson, C.C., Wild, A., Domeneghetti, A., Polderman, A., Votsis, A., Pulvirenti, B., Basu, B., Thomson, C., Panga, D., Pouta, E., Toth, E., Pilla, F., Sahani, J., Ommer, J., El Zohbi, J., Munro, K., Stefanopoulou, M., Loupis, M., Pangas, N., Kumar, P., Debele, S., Preuschmann, S., Zixuan, W., 2020. A review of hydro-meteorological hazard, vulnerability, and risk assessment frameworks and indicators in the context of nature-based solutions. Int. J. Disaster Risk Reduc. 50, 101728 https://doi.org/10.1016/j.ijdrr.2020.101728.
Shah, M.A.R., Xu, J., Carisi, F., De Paola, F., Di Sabatino, S., Domeneghetti, A., Gerundo, C., Gonzalez-Ollauri, A., Nadim, F., Petruccelli, N., Polderman, A., Pugliese, F., Pulvirenti, B., Ruggieri, P., Speranza, G., Toth, E., Zieher, T., Renaud, F. G., 2023. Quantifying the effects of nature-based solutions in reducing risks from hydrometeorological hazards: examples from Europe. Int. J. Disaster Risk Reduc. 93, 103771 https://doi.org/10.1016/j.ijdrr.2023.103771.
Su, S., Pi, J., Wan, C., Li, H., Xiao, R., Li, B., 2015. Categorizing social vulnerability patterns in Chinese coastal cities. Ocean Coast Manag. 116, 1–8. https://doi.org/10.1016/j.ocecoaman.2015.06.026.
Sun, Landong, Tian, Z., Zou, H., Shao, L., Sun, Laixiang, Dong, G., Fan, D., Huang, X., Frost, L., James, L.-F., 2019. An index-based assessment of perceived climate risk and vulnerability for the urban cluster in the Yangtze River Delta region of China. Sustainability 11, 2099. https://doi.org/10.3390/su11072099.
Sun, R., Gong, Z., Guo, W., Shah, A.A., Wu, J., Xu, H., 2022. Flood disaster risk assessment of and countermeasures toward Yangtze River Delta by considering index interaction. Nat. Hazards 112, 475–500. https://doi.org/10.1007/s11069-021-05189-4.
Syvitski, J.P.M., Kettner, A.J., Overeem, I., Hutton, E.W.H., Hannon, M.T., Brakenridge, G.R., Day, J., Vörösmarty, C., Saito, Y., Giosan, L., Nicholls, R.J., 2009. Sinking deltas due to human activities. Nat. Geosci. 2, 681–686. https://doi.org/10.1038/ngeo629.
Tessler, Z.D., Vörösmarty, C.J., Grossberg, M., Gladkova, I., Aizenman, H., Syvitski, J.P. M., Foufoula-Georgiou, E., 2015. Profiling risk and sustainability in coastal deltas of the world, 1979 Science 349, 638. https://doi.org/10.1126/science.aab3574. LP – 643.
The CPC Central Committee, P., 2019. General Office of the State Council, P. Outline of the Yangtze River Delta Regional Integrated Development Plan [WWW Document]. URL. http://www.gov.cn/zhengce/2019-12/01/content_5457442.htm. accessed 4.20.22.
The World Bank, 2015. East Asia's Changing Urban Landscape: Measuring a Decade of Spatial Growth, East Asia's Changing Urban Landscape: Measuring a Decade of Spatial Growth. https://doi.org/10.1596/978-1-4648-0363-5.
Towfiqul Islam, A.R.M., Talukdar, S., Mahato, S., Kundu, S., Eibek, K.U., Pham, Q.B., Kuriqi, A., Linh, N.T.T., 2021. Flood susceptibility modelling using advanced ensemble machine learning models. Geosci. Front. 12, 101075 https://doi.org/10.1016/J.GSF.2020.09.006.
Twilley, R.R., Bentley, S.J., Chen, Q., Edmonds, D.A., Hagen, S.C., Lam, N.S.-N., Willson, C.S., Xu, K., Braud, D., Hampton Peele, R., McCall, A., 2016. Co-evolution of wetland landscapes, flooding, and human settlement in the Mississippi River Delta Plain. Sustain. Sci. 11, 711–731. https://doi.org/10.1007/s11625-016-0374-4.
van Vliet, M.T.H., Jones, E.R., Flörke, M., Franssen, W.H.P., Hanasaki, N., Wada, Y., Yearsley, J.R., 2021. Global water scarcity including surface water quality and expansions of clean water technologies. Environ. Res. Lett. 16, 024020 https://doi.org/10.1088/1748-9326/ABBFC3.
Vicente-Serrano, S.M., Beguería, S., López-Moreno, J.I., 2010. A multiscalar drought index sensitive to global warming: the standardized precipitation evapotranspiration index. J. Clim. 23, 1696–1718. https://doi.org/10.1175/2009JCLI2909.1.
Wang, Z., Lai, C., Chen, X., Yang, B., Zhao, S., Bai, X., 2015. Flood hazard risk assessment model based on random forest. J. Hydrol. (Amst.) 527. https://doi.org/10.1016/j.jhydrol.2015.06.008.
WorldPop, 2018. The Spatial Distribution of Population in 2020 China [WWW Document]. WorldPop. University of Southampton; Department of Geography and Geosciences, University of Louisville; Departement de Geographie, Universite de Namur) and Center for International Earth Sc. https://doi.org/10.5258/SOTON/WP00670. www.worldpop.org-SchoolofGeographyandEnvironmentalScience.
Xianwu, S., Ziqiang, H., Jiayi, F., Jun, T., Zhixing, G., Zhilin, S., 2020. Assessment and zonation of storm surge hazards in the coastal areas of China. Nat. Hazards 100, 39–48. https://doi.org/10.1007/s11069-019-03793-z.
Xinliang, X., 2017. China Gridded Geographically Based Economic Data 2019 [WWW Document]. Data Registration and Publishing System of Resources and Environment Science and Data Center, Chinese Academy of Sciences. https://doi.org/10.12078/2017121102.
Xu, Y., Zhang, B., Zhou, B.T., Dong, S.Y., Yu, L., Li, R.K., 2014. Projected flood risks in China based on CMIP5. Adv. Clim. Change Res. 5, 57–65. https://doi.org/10.3724/SP.J.1248.2014.057.
Yang, L., Scheffran, J., Qin, H., You, Q., 2015. Climate-related flood risks and urban responses in the Pearl River Delta, China. Reg. Environ. Change 15, 379–391. https://doi.org/10.1007/s10113-014-0651-7.
Yang, X., Lin, L., Zhang, Y., Ye, T., Chen, Q., Jin, C., Ye, G., 2019. Spatially explicit assessment of social vulnerability in coastal China. Sustainability 11, 5075. https://doi.org/10.3390/su11185075.
Yin, J., Jonkman, S., Lin, N., Yu, D., Aerts, J., Wilby, R., Pan, M., Wood, E., Bricker, J., Ke, Q., Zeng, Z., Zhao, Q., Ge, J., Wang, J., 2020. Flood risks in sinking delta cities: time for a reevaluation? Earth's Future 8. https://doi.org/10.1029/2020EF001614.
Yin, J., Yin, Z., Xu, S., 2013. Composite risk assessment of typhoon-induced disaster for China's coastal area. Nat. Hazards 69, 1423–1434. https://doi.org/10.1007/s11069-013-0755-2.
Yu, Q., Lau, A.K.H., Tsang, K.T., Fung, J.C.H., 2018. Human damage assessments of coastal flooding for Hong Kong and the Pearl River Delta due to climate change-related sea level rise in the twenty-first century. Nat. Hazards 92, 1011–1038. https://doi.org/10.1007/s11069-018-3236-9.
Zhang, Q., Gu, X., Singh, V.P., Xiao, M., 2014. Flood frequency analysis with consideration of hydrological alterations: changing properties, causes and implications. J. Hydrol. (Amst.) 519, 803–813. https://doi.org/10.1016/j.jhydrol.2014.08.011.
Zhang, W., Xu, Y.J., Guo, L., Lam, N.S.N., Xu, K., Yang, S., Yao, Q., Liu, K. biu, 2022. Comparing the Yangtze and Mississippi River Deltas in the light of coupled natural-human dynamics: lessons learned and implications for management. Geomorphology 399, 108075. https://doi.org/10.1016/J.GEOMORPH.2021.108075.
Zhang, Y., Fan, G., He, Y., Cao, L., 2017. Risk assessment of typhoon disaster for the Yangtze River Delta of China. Geomatics, Nat. Hazards Risk 8, 1580–1591. https://doi.org/10.1080/19475705.2017.1362040.
Zhao, Q., Pan, J., Devlin, A., Xu, Q., Tang, M., Li, Z., Zamparelli, V., Falabella, F., Mastro, P., Pepe, A., 2021. Integrated analysis of the combined risk of ground subsidence, sea level rise, and natural hazards in coastal and delta river regions. Rem. Sens. 13, 3431. https://doi.org/10.3390/rs13173431.
Zhou, M., Kuang, Y., Ruan, Z., Xie, M., 2021. Geospatial modeling of the tropical cyclone risk in the Guangdong Province, China. Geomatics. Nat Hazards Risk 12, 2931–2955. https://doi.org/10.1080/19475705.2021.1972046.
Zhu, Y., Tao, S., Sun, J., Wang, X., Li, X., Tsang, D.C.W., Zhu, L., Shen, G., Huang, H., Cai, C., Liu, W., 2019. Multimedia modeling of the PAH concentration and distribution in the Yangtze River Delta and human health risk assessment. Sci. Total Environ. 647, 962–972. https://doi.org/10.1016/j.scitotenv.2018.08.075.
UNDRR, 2015. Sendai Framework for Disaster Risk Reduction 2015 - 2030. In UNDRR (Ed.). UN World Conference on Disaster Risk Reduction. Sendai, Japan. United Nations Office for Disaster Risk Reduction. URL http://www.wcdrr.org/uploads/Sendai_Framework_for_Disaster_Risk_Reduction_2015-2030.pdf, checked on 18.12.2023.